RSC Advances

REVIEW

View Article Online
View Journal | View Issue

Multicomponent nanoarchitectures for the design of optical sensing and diagnostic tools

Cite this: *RSC Adv.*, 2014, **4**, 916

Thanh-Dinh Nguyen*[a] and Thai-Hoa Tran[b]

Simultaneous integration of multifunctional properties from different components into a hybrid nanostructure with hierarchical organization is attractive to construct new materials sought for diverse useful applications. This review highlights recent advances in the fabrication of multicomponent organic-conjugated inorganic nanoarchitectures and their potential uses in optical sensing and diagnostic tools. The similarity of the particle sizes, between inorganic hybrids and biomolecules, is the reason they can integrate into new bioconjugated nanocomposites. These multifunctional properties enable such materials to function as dual diagnostic and therapeutic agents in imaging-guided therapy. Deoxyribonucleic acid (DNA)-templated replica approaches for fabricating DNA-functionalized plasmonic nanoarchitectures are discussed to show how incorporation of metal clusters onto helical DNA structures occurs. The resulting helix plasmonic assemblies response enhanced plasmonic properties and circular dichroism signals to external environments, means they can function as highly selective bioprobes. Nanocrystal superlattices are prepared by assembling the uniform colloids by guiding the external magnetic field and solvent evaporation. The highly organized superlattices with long-range ordering exhibit optical properties tuned by external stimuli and, consequently they can be useful for desirable optical sensors and photoswitchable patterns. The efforts discussed in this review are expected to present the structural diversity of promising multifunctional nanoarchitectures for the design of efficient optical sensing and diagnostic tools.

Received 1st August 2013
Accepted 8th October 2013

DOI: 10.1039/c3ra44056g

www.rsc.org/advances

1. Introduction

Recent progress in the invention and fabrication of multicomponent organic-conjugated inorganic nanostructures with hierarchical geometries has found potential applications in the design of optical sensors and diagnostic tools.[1,2] Coupling of single components, each with its different functionalities, into a nanostructure can provide new materials with entirely collective properties.[3,4] The nanostructures with hierarchical geometries, such as dumbbell, core–shell, chirality suprastructure, and photonic assemblies, can provide new tunable physical properties in response to external stimuli.[5–8] Given that such promising materials exhibit unique properties, further application

[a]*Department of Chemical Engineering, Laval University, Quebec G1V 0A6, Canada. E-mail: thanh-dinh.nguyen.1@ulaval.ca*

[b]*Department of Chemistry, College of Sciences, Hue University, Hue 84054, Vietnam*

Thanh-Dinh Nguyen completed his BS (2003) and MS (2006) degrees in chemistry from Hue University, Vietnam. He moved to Canada, joined the laboratory of Prof. Trong-On Do at Laval University in 2007, and completed his PhD degree in 2011 in chemical engineering. His research interests are focused on the shape-controlled synthesis and self-organization of colloidal nanostructures.

Thai-Hoa Tran received his BS (1980) and PhD (2001) degrees in chemistry from Vietnam National University – Hanoi. Prof. Tran is currently the Dean of the physical chemistry laboratory, College of Science, Hue University. His research interests include carbohydrate derivatives, DNA-conjugated hybrid nanostructures, and mesoporous materials.

options for the hybrid-based nanoarchitectures appear to be endless.

Two main routes are used to synthesize the hybrid (Janus) nanostructures. Controlled growth of the metal particles on the semiconductor seeds by light irradiation is an effective synthetic route for plasmonic semiconducting Janus particles.[3,9] Decomposition and reduction of secondary precursors on supports are both applied for synthesizing metal/oxide nanohybrids with linker molecules through directed attachment.[5,10] The formation of either core–shell or dumbbell geometries of a Janus structure is dependent on the structural lattice of the particles.[11] The understanding of particle–particle interactions of a hybrid system provides a programmable approach to fabricate Janus particles with tailor-made properties.

Deoxyribonucleic acid (DNA) is a responsive chiral suprastructure compatible with biomedicine. DNA nanotechnology is a rapidly developing research area in nanoscience. DNA used as an intriguing soft matter template to build plasmonic cluster-functionalized DNA nanoarchitectures with assembled ordering over large domains is a interesting research direction for materials scientists.[1,12] DNA has the possibility to integrate its chiral property within the nanoscale DNA-functionalized plasmonic assemblies, while a plasmonic enhancement of the electronic field is typically observed in the complex structures by dipolar coupling of the particle assembly. This feature makes such materials possibly provide simultaneous light–matter interaction optical responses and surface enhanced Raman scattering (SERS) signals.[13,14]

Surface functionalization of the nanostructures with appropriate hydrophobic, hydrophilic stabilizers, and silica layers can produce coated colloids in process to self-organize into periodic superlattice structures.[15,16] The ordered hierarchical nanocrystal arrays can appear iridescent and have an enhanced SERS signal in case of the plasmonic assemblies, accompanied with peak reflected wavelength tuned by changing external stimuli.

The advance of the synthetic methods for the organic-conjugated inorganic nanoarchitectures has paved the way toward the design of imaging-guided therapeutics and optical sensing devices. Discussions of the advanced pathways as an interdisciplinary research direction are beyond the scope of the present article, but some applied fields and current topics of these researches are highlighted:

• The complex nanostructures used for cancer diagnostics and therapeutics have emerged as a potentially powerful branch of research activity. The size of the inorganic particles is smaller than 100–10 000 times that of the cells, thus smart nanodrugs can be obtained by bioconjugating the particles with cargoes of targeting moieties and therapeutic agents. The bioconjugated structures hold great potential for biomedical applications because of the capacity of targeted delivery into the cancer cell membranes in response to photon excitation or a magnetic field.[17] Needless to say, the development of multimodal imaging techniques based on such smart nanomaterials capable of accurately detecting cancer tumors is much needed in clinical medicine. The plasmonic–magnetic and fluorescent–magnetic nanohybrids are known as promising bifunctional nanomaterials for cancer diagnosis acting through scattering of plasmon and intense emission alongside magnetic contrast, respectively.[18–20] Recent research has revealed that lanthanide-doped $NaYF_4$ luminescence upconverting nanostructures are promising agents for highly efficient diagnosis and therapy platforms arising from the possibility of releasing reactive singlet oxygen species to kill the cancer cells under near infrared (NIR) light irradiation.[21–23]

• Strands of short DNA chain can act as effective bricks to assemble into hierarchical three-dimensional (3-D) superlattices.[24] Recent reports demonstrate that co-assembling the plasmonic clusters with chiral DNA supramolecules can produce DNA-functionalized plasmonic nanostructures with helical organization.[13,25] The plasmonic assemblies possess enhanced collective properties different from individual components. A strong plasmonic coupling can arise from the precise control over small interparticle distances between plasmonic cluster geometries assembled on the DNA template.[26] The chiral plasmonic assemblies typically create light–matter interaction optical responses tuned by controlling shape-dependent surface plasmon energy.[27] Raman signals arising from the interaction of an analyte molecule with the assembled plasmonic particles can be accessible to the single molecules at trace amount levels.[28] Such supramolecular nanomaterials are expected to design highly sensitive SERS bioprobes for the selective detection of desirable biochemical substances.[29,30]

• The uniform particle colloids are building blocks to self-assemble into highly organized superlattices in response to a guide of the external magnetic field or slow solvent evaporation. The long-range order of the assembled superlattices can form resulting in light-reflected structures. The superlattices derived from colloidal assemblies have been particularly useful for constructing responsive photonic nanomaterials.[31,32] The superlattices can exhibit collective physical (optical, conductive) properties in response to the external stimuli of chemical change. Thus, these nanomaterials have the potential to integrate tunable reflected light functions into optical filter and switch devices.[33]

This review is focused on the structural diversity of the multicomponent organic-conjugated inorganic nanostructures that are of interest in the most intense optical sensing and imaging-guided therapeutic technologies. This motif has been considered as the most modern nanostructure research to produce a rapid diversification of covering a continuum from 3-D solid complex nanostructures: (i) organic-conjugated inorganic core–shell and dumbbell nanostructures, (ii) DNA-functionalized plasmonic suprastructures, and (iii) responsive photonic nanocrystal array assemblies. The families of the functional inorganic nanocomposites with hierarchical geometries are promising materials with the potential to open new research horizons, in the future, for sensing and medical applications.

Herein, the author gives an overview of functional hierarchical nanocomposite systems with state-of-the art in nanoscale synthesis. The review presents the synthesis and applications of these novel materials, covering solution-based synthetic methods to produce diverse materials with specific structures

and morphologies then pioneering innovative appplications in optical sensing and biomedicine. The unique multifunctional properties and potential applications of such promising materials are highlighted through clear examples in the Introduction and Perspective sections. Next, synthetic approaches including surface growth for Janus nanoparticles, templated assembly of plasmonic cluster-attached DNA helices, and external magnetic field-guided colloidal assembly and evaporation-induced self-assembly (EISA) for superlattices are presented and how the boundary of each method acts to control the reaction mechanisms behind the formation of the multicomponent nanoarchitectures is discussed. We highlight the behaviours of the desired morphology of these well-defined nanomaterials dependent on the reaction parameters. Eventually, we demonstrate how such promising materials with tailor-made properties are useful for the design of optical sensing and imaging-guided therapeutic tools.

2. Perspectives of multicomponent nanoarchitectures

Compared to single nanoparticles, complex interparticle interactions presented in the nanohybrids can lead to collective physical properties that are distinct from simply the sum of those of the two particle constituents.[34] Different potential applications of the multicomponent nanostructures with hierarchical geometries are shown in Fig. 1. Biological molecules, such as DNA, antibodies, proteins, peptides, immobilized on inorganic nanocomposite supports through physical adsorption, electrostatic binding, and covalent coupling can generate biofunctional nanocomposites. The biomolecule-modified nanohybrid conjugates are used for numerous biotechnological applications in biosensors, biofuel cells, and affinity cell separations.[35] Advances in synthetic methods of DNA preparation have enabled the construction of efficient bioprobes through the incorporation of plasmonic clusters within DNA supramolecules. Otherwise, tunable light sources are essential for information technologies.[36–38] The superlattice materials are generally prepared by self-assembling uniform particle colloids by means of the application of an external magnetic field and EISA. The long-range order organized in the superlattices can offer the possibility to manipulate light by prohibiting propagation of certain wavelengths, thus generating structural colors.[39,40] The tunability of the photonic band-gap of the host structure in the visible region is attractive for photoswitchable patterns.[41–43]

Gold nanoparticles were first studied on immunogold biolabeling due to their superior optical properties.[45] Later, fluorescent-biolabelling properties of quantum dots were reported to overcome the limited success with traditional organic and encoded fluorophores.[46,47] Taking advantage of near-infrared over visible light excitation for diagnostic and therapeutic bifunctional materials for cancer treatment, integrated plasmonic–magnetic, fluorescent–magnetic, and fluorescent-upconverting nanocomposites have been considered promising.[48–51] Another concept, co-assembly of the DNA template with plasmonic clusters on appropriate substrates can produce DNA-functionalized plasmonic supramolecular nanostructures with enhanced plasmonic and circular dichroism signals, thus the resulting materials are designed as optical sensing nanoprobes in response to external biochemical stimuli.[13,27,52] Since the landmark work in 1996 demonstrating the attachment of thiolated DNA to gold particles,[53] interest in DNA-based bio–nanotechnology has expanded significantly because of its applications ranging from sensitive biosensing, particle

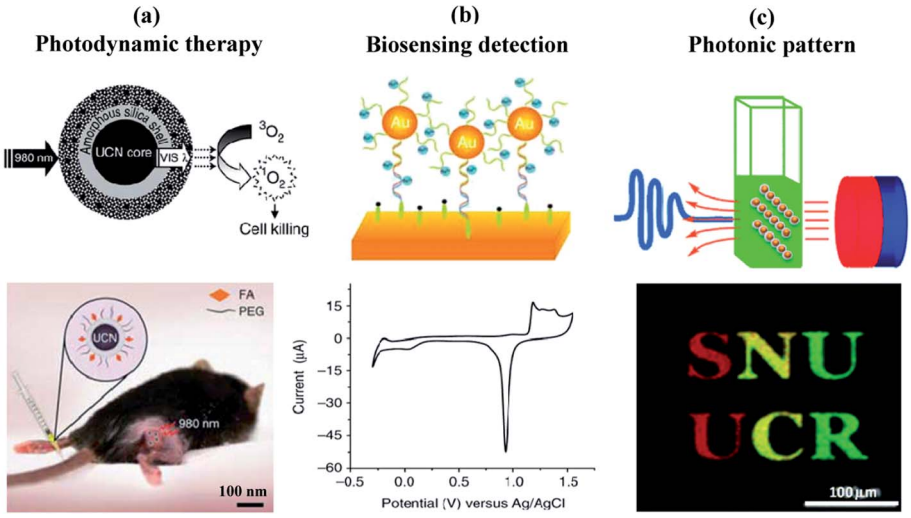

Fig. 1 Perspective and modern applications of multicomponent nanoarchitectures in nanotechnology. (a) Oxygen singlet-released photodynamic therapy in a mouse melanoma model using mesoporous silica-coated upconverting particles. Reproduced with permission from ref. 82. Copyright 2012 Nature Publishing Group. (b) Au particle-based DNA sensors for the detection of DNA obtained by the hybridization of the Au particles loaded with bioprobes as presented in a cyclic voltammogram for an Au electrode in H_2SO_4 solution. Reproduced with permission from ref. 27. Copyright 2012 Nature Publishing Group. (c) Self-organization of magnetic cluster colloids into photonic nanoarray patterns upon applying an external magnetic field. Reproduced with permission from ref. 44. Copyright 2009 Nature Publishing Group.

assembly, and gene and drug delivery. Incorporation of the photonic nanocrystal assemblies into polymer hosts is carried out to build sensitively photoswitchable patterns with photonic properties tuned by the external environment.[54]

Despite substantial recent progress in the invention and fabrication of highly selective nanomaterials for modern applications, challenging problems have arisen for materials scientists. The targeted delivery of the biomolecule-conjugated inorganic nanocomposites to cancer solid tumors is one of the most important problems in cancer medicine. The toxicity of byproducts of the cancer treatment generated by biofunctional nanocarriers is the major challenge facing biomaterials researchers. The high cost of using the DNA supramolecule template to fabricate optical sensing bioprobes could make it difficult to transfer to development and commercial production. The fabrication of periodic nanocrystal arrays with photonic properties dispersed in solvent is often limited to only magnetic particles, while other properties of photoswitchable patterns, such as plasmonic and semiconducting particles, meet requirements for photoelectronic device designs on scale-up. Finding the best solutions to overcome these barriers is a gold key to ongoing research on the unique properties of such promising functional nanomaterials.

3. Synthetic concepts

3.1. Surface growth

Surface growth developed for nanoparticle synthesis is a long way from being commonly used in materials research. One of the first examples is the synthesis of gold nanorods, the surface growth is composed by generating gold seeds in the early stages followed by rod-shape growth, in which the aspect ratio can be tuned by varying the metal salt/seed ratio.[45] This procedure has been improved by other research groups. For example, Ye *et al.*[55] reported an improved seed-mediated growth for the synthesis of gold nanorods through the use of aromatic additives. The addition of aromatic compounds such as salicylic acid in the synthetic solution resulted in significantly reducing the CTAB surfactant concentration and generated gold nanorods with longitudinal surface plasmon resonance. The authors pointed out that the use of binary CTAB and sodium oleate surfactant allowed the improvement of the dimensional tunability and monodispersity of the gold nanorods.[56] Alternatively, an another synthetic direction reported by Gao *et al.*,[57] who used a hard template of silica nanotubes to fabricate metal (Au, Ag, Pt, Pd) nanorods. The reduction and seeded growth of the metals occurred inside the amino-functionalized silica nanotubes and, consequently the metal nanorod replicas were obtained after etching of the silica shell template.

Later, surface growth has been extended to complex Janus nanostructures.[58] Fig. 2 shows two routes of surface growth including photodeposition and chemical attachment for these materials. Under appropriate reaction conditions, the nanohybrids with core–shell and dumbbell geometries can form by sequentially heterogeneous growth of secondary components on preformed seeds with or without linker molecules through directed attachment.

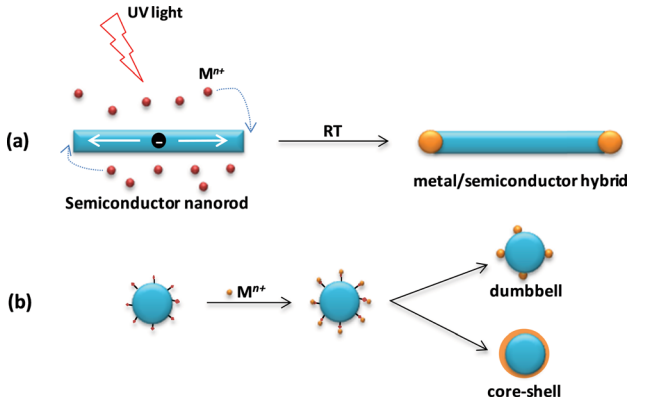

Fig. 2 Surface growth routes of (a) photodeposition and (b) chemical attachment for the synthesis of the inorganic Janus nanoparticles.

UV light-induced growth is considered as a powerful tool to synthesize a family of plasmonic semiconducting nanohybrids without the aid of organic molecular bridges (Fig. 2a). Mokari *et al.*[59] first proposed a light-induced growth mechanism for the formation of Au/CdSe nanohybrids, where electrons are generated on the CdS semiconductor surface under UV excitation and then dominantly migrated to tips of the CdS nanorods due to different facet energies. This leads to the Au clusters being formed to escape to the solution as free Au ions by releasing these electrons. The reduction of the Au ions occurs at the tips of the CdS rod seeds to form Au clusters located at these tips. The electrons released from the CdS tips transfer to the Au clusters to continuously reduce Au ions in the reaction solution resulting in the growth of larger Au particles. This migration of Au particles can be attributed to higher surface energies on the tips of the nanorod. Thus, the rod tips are preferential growing sites for the Au particles, resulting from more accessible sites on the tips, where the surfactant capping is weak. The successful synthesis of these materials *via* a light-induced growth approach is a breakthrough for the later extent of different plasmonic semiconducting nanohybrids. This synthetic method allows not only the control of the population of uniform metal clusters on each individual semiconductor surface but also to control the particle size and distribution. Dinh *et al.*[60] also applied this photo-irradiation technique for the deposition of silver clusters on the titania nanocrystals without the aid of the capping linkers and the resulting Ag/TiO_2 hybrid nanomaterials exhibited much higher catalytic activity than commercial catalysts arising from the coupling of the plasmonic semiconducting properties of silver and titania particles in a Janus nanosystem.

The second route is the growth of the secondary precursors on the non-semiconducting oxide nanocrystal seeds with the aid of organic linkers through different chemical reactions, such as reduced precipitation, ionic exchange deposition, surface adsorption, and surface-activated functionalization (Fig. 2b). The colloidal nanohybrids are generated upon reaction of molecular precursors in liquid solution in the presence of the surfactants. Once the synthesis is activated at a suitable temperature, monomers are generated, which then induced the

nucleation of the nanoparticles and sustain their subsequent enlargement. The organic molecular bridges are important along the courses of the hybrid formation. The selection of the suitably-structured element correlated with electron-transferred capacity at the interface of components is critical for the design of the hybrid nanostructures.

One of the first examples of the synthesis of gold–iron oxide core–shells was reported by Shevchenko *et al.*[61] through thermolysis of $Fe(CO)_5$ at the gold particle surface in an octadecene–oleylamine–oleic acid mixture. The core–shell hybrids were formed by depositing a metallic iron shell around a gold core and subsequent oxidizing of the iron shell to form an iron oxide hollow. In a continuing study for this material, Yu *et al.*[62] synthesized Au–Fe_3O_4 dumbbells with controlled sizes by thermolysis of $Fe(CO)_5$ on gold particles and subsequent oxidation in 1-octadecene. This chemical deposition route is sensitive to the nature and concentration of the organic linkers. The size and distribution of the deposited particles can be controlled by choosing appropriate organic linkers. In this case, controlled heterogeneous growth of the iron precursors on the gold seeds was associated with the particles/capping agents ratio and temperature of deposited precursor injection. Nguyen *et al.*[63,64] used bifunctional organic linkers, aminohexanoic acid and hexamethylenediamine, as capping agent and bridge, for the synthesis of diverse capped oxide nanocrystals and subsequent deposition of the plasmonic (Au and Ag) clusters on the oxide supports. This technique guarantees preferential heterogeneous growth of the metal precursors on the support surface *via* interaction between metallic precursors and uncoordinated carboxylic or amine groups of bifunctional ligand-capped oxide nanocrystals. Recently, the liquid exchange process was reported by Dinh *et al.*[65] on the fabrication of mesoporous Ag/TiO_2 nanodisks with enhanced photocatalytic activity.

In Section 4.1, the synthesis of a variety of the inorganic Janus nanoparticles by using the surface growth routes is presented. The hybrid nanomaterials are divided into two groups composed of dumbbell and core–shell geometries. The size and shape control and new collective properties followed by useful applications of these materials are mentioned as well.

3.2. Plasmonic clusters assembled with DNA

DNA, a genetic biomaterial in the cells, is composed of complementary binding of A with T and C with G associated with supramolecular forces leading to the formation of a helical structure of double-stranded DNA.[66] The helical structure made DNA has specific biological functions.[67] The unique inherent properties of DNA have inspired scientists to discover and synthetically fabricate the self-assembly of the inorganic precursors with DNA to build 2-D and 3-D nanostructures with controlled shapes.[68,69] Organic ligand-assisted synthesis is a powerful tool for the formation of monodisperse colloidal inorganic particles. The organic ligands not only contribute to the stability of the particles in the solution by capping on its surfaces, but also provide the surface functionalities for the assembly into architectural structures. As electronic-rich structures, DNA inherently is constituted of nitrogenous bases and anionic phosphate groups with an affinity for metals. DNA at one end is oligonucleotide functionalized with a thiol group that could be used to bind with metal clusters, while rendering ends of DNA ligands freely dispersed in the solution. Given that DNA can serve as either stabilizing ligand or structural template for the metal clusters.

Much recent progress in the construction of plasmonic particles functionalized or templated by DNA has been achieved, consequently diverse organized structures at nanoscale size can be obtained with different well-defined shapes, particularly the resulting helical hybrid nanostructures are a witness of the DNA helix templation. Fig. 3 shows two main strategies for the self-assembly of the metal particles with DNA. The metal/DNA hybrid nanostructures were initially prepared and then assembled into the organized structures by linking chemistry. An another route is to directly prepare the assembled metal particles templated by DNA bundles.

Selective hybridization of the prepared metal particles with the DNA ligands can occur by either ligand exchange or attachment reaction. The hierarchical shape of the assembled metal particles is often determined by position and electronic density of the functional surface groups and the geometry of DNA. The pioneering work of Park *et al.*[53] introduced the first examples of the functionalization of Au particles with oligonucleotides through the formation of binding between alkanethiol groups at the ends of DNA with citrate-stabilized Au particles. An excess amount of the DNA linkers was added to a DNA-functionalized Au nanohybrid aqueous dispersion to link these nanohybrids by further DNA hybridization. This reversible supermolecular assembly can be controlled by reaction temperature to yield desired gold/DNA macroscopic networks.

Advances in DNA nanotechnology offer possibility of the production of commercial DNA bundles with helical superstructures.[69] The DNA bundles are ideal platforms to template the assembled plasmonic particles. The constant distances between particles could be fixed on flexible DNA helical strands to induce their plasmonic properties different from the metal particle assemblies by solvent evaporation.[8] The successful synthesis of such novel materials was a breakthrough for the extended development of biodetection systems. This straightforward synthetic procedure had been latter extended to diverse inorganic nanoparticles. In Section 4.2, co-assembly of the plasmonic clusters with supramolecules and helical template bundles of DNA is presented. These sections also include the unique properties and optical sensing applications of the resulting plasmonic cluster-functionalized DNA nanostructures.

3.3. Assembling colloids into superlattices

The uniform inorganic nanoparticle colloids behave like well-defined molecules to arrange the orientational order into a superlattice.[70,71] The highly organized superstructures of the particle assemblies provide new materials with collective physical properties resulting from coupling of the individual particles.[72,73] The self-assembly of the particle colloids in the solution is a fundamental behavior by themselves as they

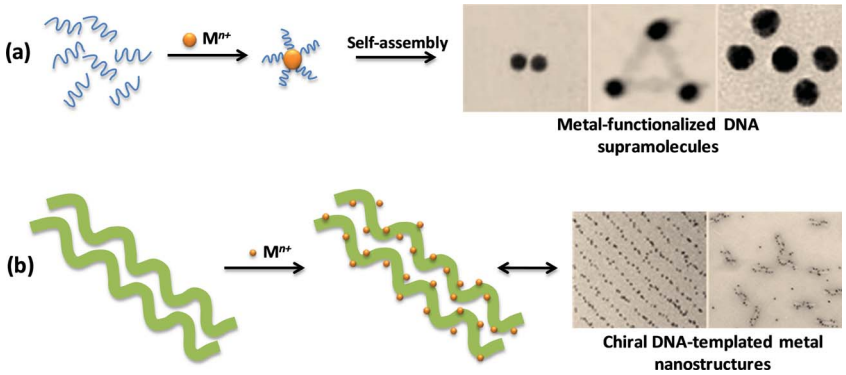

Fig. 3 Self-organization of DNA with plasmonic particles. (a) Plasmonic particle-functionalized DNA supramolecules. Reproduced with permission from ref. 52. Copyright 2013 American Chemical Society and (b) plasmonic particle-functionalized DNA helix bundles. Reproduced with permission from ref. 13. Copyright 2011 Nature Publishing Group.

involve various interactions between particles, capping molecules, and solvent. The physical properties of the assembled materials can be tuned by controlling the particle size, surface chemistry, and external stimuli.

The good stability of the uniform particle colloids in the solution is an important factor for the controlled assembly process. To address this issue, chemistry functionalization of the inorganic particles is performed to modify the particle surface in order to be compatible with the assembly environment. The particle colloids as building blocks can organize into a periodic superstructure by either applying external stimuli or interfacial assembly when the balance of the repulsive, attractive, and dipole–dipole forces of the surface-modified particles can be established in the solution. The driving force of the particles organized in a superlattice is associated with relatively weak attraction forces between particles in the solution upon self-assembly.

The Yin group[74,75] pioneered the application of an external magnetic field to surface-modified superparamagnetic Fe_3O_4 cluster colloids to self-assemble into periodic superlattice nanoarrays dispersed in solution. This robust procedure is composed of two steps: (i) initial aqueous preparation of uniform polyacrylate-capped Fe_3O_4 clusters followed by coating the polyacrylate-capped Fe_3O_4 nanoclusters with a silica layer in case of the assembly employed in non-aqueous media and (ii) self-organization of these surface-modified magnetite clusters into photonic nanocrystal arrays upon applying the external magnetic fields. Fig. 4 shows two main routes for the self-organization of the surface-modified magnetite clusters into photonic nanocrystal arrays by means of application of the external magnetic field.

Self-assembly of the magnetic clusters employed in water, the authors synthesized uniform Fe_3O_4 clusters by hydrolyzing $FeCl_3$ in a polyacrylic acid/diethylene glycol basic aqueous solution at 220 °C.[74] The polyacrylate bound to the particle surface through coordination of the carboxylate groups with iron cations, whereas the noncoordinated carboxylate groups on the polymer chains exposed to the aqueous solution rendered the particle surfaces highly charged. Thus, after the extra surfactant was removed and the ionic strength was decreased by centrifugation, the polyacrylate-capped Fe_3O_4 clusters can be well-dispersed in the aqueous solution for several months. For self-assembly in nonpolar solvents, the authors achieved a coating of the polyacrylate-capped Fe_3O_4 nanoclusters with a silica layer.[75] The polyacrylate-capped clusters grafted with an alkoxysilane monolayer through silylation sol–gel reaction rendering them soluble in the nonpolar phase. Through a careful balance of the repulsive electrostatic force of these colloidal clusters and magnetically induced attractive forces, the polyacrylate-capped Fe_3O_4 clusters and polyacrylate-stabilized Fe_3O_4 clusters coated with silica can assemble in water in linear chains with periodic interparticle spacing referred to as colloidal photonic nanocrystal arrays upon applying the external magnetic field.

The photonic magnetic superlattices retained their superparamagnetic property at room temperature and exhibited higher saturation of magnetization. Taking advantage of applying a simple external magnetic field over a conventional method such as EISA, the periodically organized nanostructures with photonic properties dispersed in the solution offered rapid, reversible tuning over the entire visible spectrum using the external magnetic field. These materials can reflect with incident light at a specific diffraction wavelength tuned by controlling the strength of the external magnetic field. Consequently, monochromatic colors of these photonic materials can appear across the entire visible spectrum. Fully reversible optical responses to changes in the external magnetic field make such materials useful in the design of the photoswitchable patterns.

In an another approach, multi-dimensional superlattices can be obtained by EISA of the colloidal dispersion. The particle assembly typically occurs at the plane liquid–liquid interface, giving to rise homogenous particle networks or composite organic–inorganic films with long-range ordering.[72] Upon EISA, the different orientations and packing structures of the particles can be generated by controlling the thickness of the surface passivation layer, particle sizes, surface pressure, and solvent evaporation rates. Recent attempts have used bottom-up approaches of self-organization to synthesize a variety of superlattices. Ye *et al.*[76] used the interfacial assembly method to achieve ordered nanocrystal assemblies from uniform

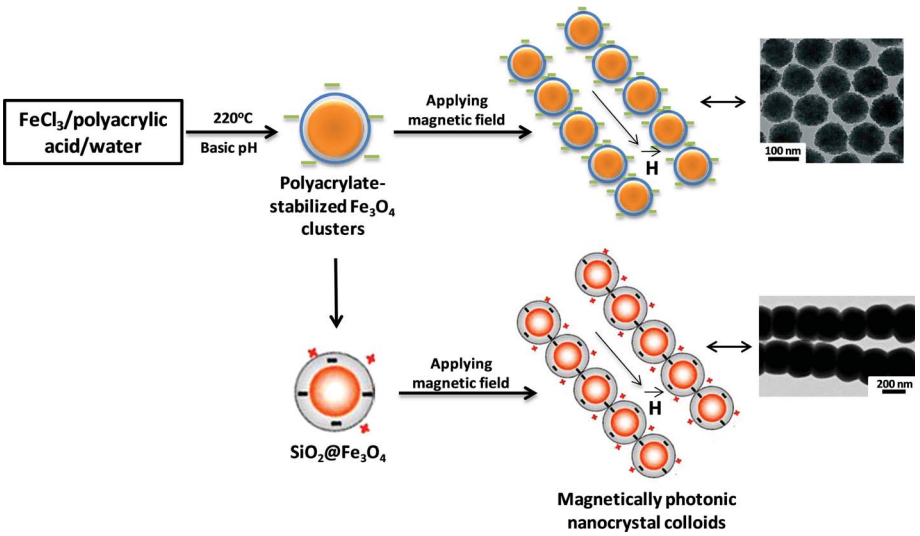

Fig. 4 Self-organization of negatively charged polyacrylate-capped Fe_3O_4 clusters and positively charged silica-coated polyacrylate-capped Fe_3O_4 clusters into periodically photonic nanocrystal arrays in response to external magnetic fields. Reproduced with permission from ref. 74. Copyright 2008 Wiley-VCH and reproduced with permission from ref. 54. Copyright 2007 American Chemical Society.

upconverting β-$NaYF_4$ nanophosphor colloids prepared by thermal decomposition of sodium and lanthanide trifluoroacetates dissolved in an oleic acid and 1-octadecene mixture. The hexane dispersion of the β-$NaYF_4$ nanorods was dropcast onto the ethylene glycol (EG) surface and allowed the solvent to slowly evaporate, large-area, continuous, uniform β-$NaYF_4$ nanorod superlattice films with controlled layer domains can be obtained (Fig. 5a). The organized superlattices showed strongly birefringent textures observed under crossed polarizers due to the long-range order of the nanorods, which is comparable to the optical properties of the liquid crystals (Fig. 5b).[78,79]

Substantial recent progress in the incorporation of particles into the liquid crystal phase has been studied to produce liquid crystal-oriented particle assemblies.[80,81] Recently, Umadevi *et al.*[77] reported the ligand exchange of CTAB capping on the gold nanorods with nematic silane liquid crystals and their assembled nanoarrays with nematic ordering were obtained upon slow evaporation of the organic solvent. Fig. 5c shows the preparative procedure composed of two steps: the replacement of the CTAB ligand capping on the nanorod surface by a mercaptotrimethoxy silane followed by hydrolysis and condensation of trimethoxy silane groups to form an oligosiloxane

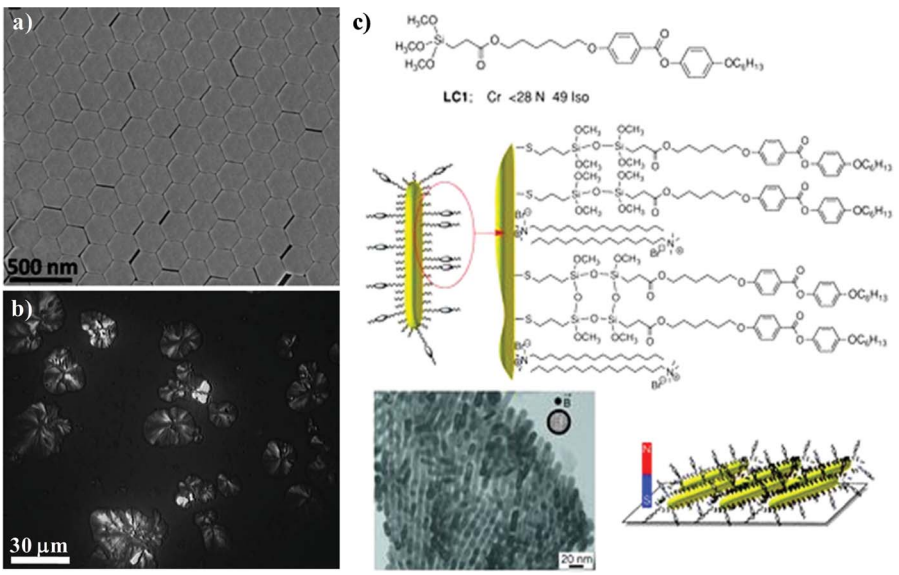

Fig. 5 Evaporation-induced self-assembly of colloidal upconverting nanophosphors into superlattices: SEM image (a) and polarized optical microscopy image (b) of the assembled superlattice of $NaYF_4$:Yb/Er hexagonal nanoplates. Reproduced with permission from ref. 76. Copyright 2010 Proceedings of the National Academy of Sciences. (c) Self-assembly of nematic liquid-crystal-functionalized gold nanorods formed upon slow solvent evaporation. Reproduced with permission from ref. 77. Copyright 2013 Wiley-VCH.

network around the gold nanorods. The gold nanorods after liquid exchange became hydrophobicity and they can easily transfer the phase from aqueous to organic solvent. The electron microscopy images of the silane-coated gold nanorod assemblies show densely packed, highly ordered 3D superstructures. Polarized optical microscopy of such samples shows birefringence and these gold nanorod arrays can be reoriented by applying an external magnetic field, demonstrating the formation of ordered liquid crystal-like anisotropic superstructures.

The magnetic field-guided colloidal assembly affords a photonic visible host of highly ordered superlattices dispersed in solvent, paving the way toward the design and imprinting of photonic composite patterns with photoswitchable properties. Otherwise self-assembly of the particle colloids upon either solvent evaporation or gravitational sedimentation typically has a tendency to form solid films of the organized superlattices, which likely offer applications for optical sensing and thermal conductivity devices. In Section 4.3, we provide an overview of the efforts in the fabrication of the ordered superlattices prepared by both applying the external magnetic field and interfacial assembly and potential uses of such novel materials in these application fields.

4. Multifunctional nanoarchitectures

4.1. Janus particles

Dumbbells. In the growth of the hybrid nanostructures, each component can fuse together to generate a dumbbell-shaped structure when the individual components involved have similarity in the crystal structures and lattice parameters.[61,82] Such a dumbbell structure constitutes a particle bound to another one and interfacial contacts between particles may be considered to be bridges to allow charged transfers across this nanoscale junction. This behavior can result in a significant change in the local electronic configuration of each single component, giving new collective properties of the nanohybrids.[5]

Materials researchers have applied the light-induced growth route for the synthesis of the plasmonic semiconducting nanohybrids through direct assembly of different components without the aid of organic molecular bridges. Fig. 6 shows the pioneering work of the Banin group,[9,83] who showed the first examples of Au–CdSe rod nanohybrids *via* selective deposition of Au clusters on the tips of CdSe nanorods under UV light irradiation. Experimental results demonstrated that anisotropic reactivity of {001} tips of CdSe/CdS nanorod seeds resulted in the growth of Au particles on only tips of the rods. Facets at the fast-growing end, which is further from the CdSe core, tend to be sulfur rich, while facets at the end closer to CdSe core tend to be cadmium rich. S–Au interactions indicate that Au deposition primarily occurred on the facets at the end from the CdSe core and subsequent deposition on the facets at the end closer to the CdSe core. Upon UV excitation, large Au domains can be exclusively deposited at one end of the CdSe/CdS rods because of electron migration to one of the tips, whereas under ambient light conditions, the deposition of Au clusters along the nanorods was strongly influenced by reaction temperature and ligand-mediated defect sites. Precise control over the deposition of the Au clusters at specific locations on the CdS core–shell nanorods would not only be critical for directed assembly, but should have the influence on the optical properties of the rods. The luminescent quenching of the Au–CdSe nanohybrids was observed owing to a strong coupling between plasmonic and semiconducting particles.

Controlled growth and reductive transformation of gold shells around pyramidal CdSe nanocrystals by either electron beam irradiation or addition of the reducing agent were reported by Meyns *et al.*[85] on the synthesis of Au–CdSe hybrids with rod and pyramid shapes. The size of deposited gold dots can be tuned from 1.4 to 3.9 nm by varying the capping ligands and CdSe shape. The rod- and pyramid-shaped CdSe particles are thermodynamically favored for size-controlled growth of Au precursors on their corners/edges and tips through the appropriate choice of metal precursor and surface ligand concentration. The pyramid structure provides sharp angles as reactive sites for the nucleation of Au particles. A similar procedure was also achieved by Chakrabortty *et al.*[86] to produce Ag_2S–CdSe/CdS hybrid nanorods with exclusive location of Ag_2S particles at the tips of the semiconductor rods. The deposition of Au and Ag precursors on the CdSe/CdS nanorods generated Au–Ag/CdSe/CdS dumbbells.

The influence of degree of mismatch between crystal lattices of two components on the hybrid shapes was studied by Shim *et al.*,[87] who examined the growth of metal sulfides on Fe_2O_3 nanospheres. The lattice mismatch of the semiconductor and iron oxide was 4.0% for ZnS, 4.6% for CdS, and 5.1% for HgS. As the amount of the lattice mismatch increased, the authors observed fewer instances of junction formation between semiconductor and magnet domain and an increasing occurrence of the homogeneous nucleation of the semiconductors. Well-controlled deposition of Au clusters on CdSe/CdS nanorods can be obtained under ambient light conditions by varying additional Au concentration. The reactivity difference of the facets at the tips and sides of the nanorods caused a change in Au-decorated geometry by adjusting Au concentration. The attachment of the Au particles on the CdSe/CdS rods at the exclusive tips showed non-epitaxial growth at the apex of the CdS shell. Liu *et al.*[88] reported the synthesis and optical properties of Ag_2S- and Ag_2Se-coated Au hybrids. These materials began by growing Au nanorods and bipyramids in aqueous media and then grew a silver layer on the seeds by reduction of silver salt at the surface. Sodium sulfide or selenourea was reacted with silver coating resulting in the conversion of silver layers into Ag_2S or Ag_2Se shells, respectively. The seed shape and shell thickness can be tuned independently, forming Ag_2S- and Ag_2Se-coated Au nanohybrids with tunable optical properties.

Metal-deposited non-semiconductor oxide nanohybrids are synthesized by decomposing organometallic precursors on seeds. Decomposing $[Fe(CO)_5]$ precursors on the Au particles in the presence of mixed oleic acid–oleylamine afforded Au–Fe_3O_4 dumbbells.[89] Metallic iron clusters grew on the Au seeds and then oxidized to Fe_3O_4 particles to form Au–Fe_3O_4 particles upon exposure to air. The oleic acid–oleylamine-capped

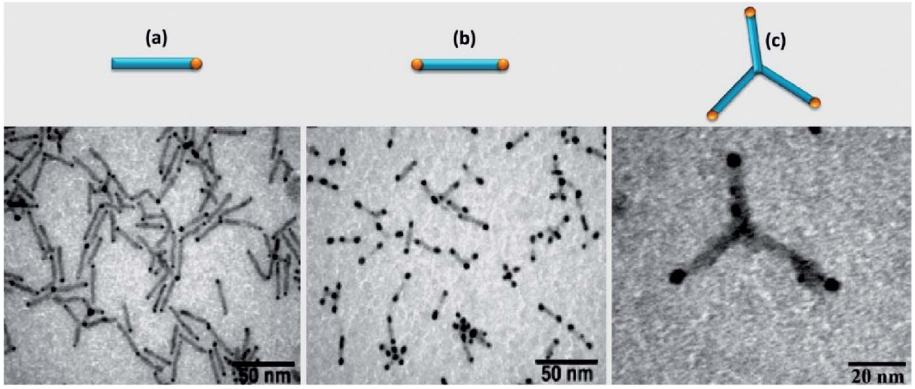

Fig. 6 Schematic illustration and TEM images showing the selective growth of Au particles onto the tips of CdSe quantum dots synthesized by selective photodeposition under UV light irradiation. (a) CdSe nanorods. (b) Au particles attached on the tips of the CdSe nanorods. (c) Au growth on the tips of CdSe tetrapods. Reproduced with permission from ref. 9. Copyright 2004 AAAS Science.

dumbbells were modified by surfactant exchange reaction to polyethylene glycol (PEG)- and HS–PEG–NH_2-conjugated Au–Fe_3O_4 hybrids. The capped Au–Fe_3O_4 dumbbells before and after surface modification both exhibited superparamagnetic properties at room temperature. The Au–Fe_3O_4 dumbbells showed a red-shifted plasmonic absorption in phosphate buffered saline at 530 nm relative to 8 nm Au particles because of junction effects in the dumbbell structure. The use of oleylamine as both reducing agent and capping agent for depositing Au clusters on Fe_3O_4 particles generated Au–Fe_3O_4 dumbbells.[90] The capped Au–Fe_3O_4 hybrids were exchanged with CTAB and sodium citrate resulting in a transfer from the organic solvent into water. The water soluble hybrids serve as seeds for further growth of Au–Fe_3O_4 hybrids with thicker Au coatings by adding $HAuCl_4$ under reductive conditions. Ag/Au–Fe_3O_4 hybrids can be obtained by adding $AgNO_3$ to the reaction solution containing the Au–Fe_3O_4 seeds under the same synthetic procedure.

A galvanic displacement process was applied for synthesizing cube-shaped plasmonic nanocages reported by Xia *et al.*[91] In an interesting report by Janet *et al.*,[84] Ru/Cu_2S hybrid nanocage analogies were synthesized by growing $Ru(acac)_3$ precursors on Cu_2S particles in octadecylamine at 210 °C. Fig. 7 shows electron microscopy images of the Ru/Cu_2S nanohybrids with single-crystalline core showing patterns of dark and light regions. Selective growth of the Ru clusters on the crystal edges of the Cu_2S nanocages resulted in a highly symmetrical cage around the Cu_2S core. The formation of the cage structure could be due to capping the thiol-passivating ligands on the Cu_2S particle facets, leading to blocking growth of these facets. The cage-shaped nanohybrids with void and high surface area are of interest to catalysis, gas storage, and drug delivery.[92] In this case, the Ru/Cu_2S nanocages can function as efficient electrocatalysts for H_2O_2 sensing with two orders of magnitude higher than Cu_2S electrodes, which is correlated to the cage shape and component combination.

Core–shells. In the synthesis of the core–shell structures, the large lattice space difference of the individual components can result in the formation of core–shell structures.[61,82] The isolation of the core from surroundings in a core–shell structure, which provides new materials and allows functionalization with other components.[93,94] Choi *et al.*[95] reported a general route for the synthesis of different metal/oxide hybrids by thermolysis of mixtures of metal–oleate (Fe, Mn) complexes and metal–oleylamine (Au, Ag, Pt, Ni) complexes in organic solvent using oleylamine capping agent. Water-soluble oligonucleotide-conjugated Au–Fe_3O_4 hybrids were prepared for multimodal biomedical probes. Au–Cu_2O core–shells with symmetrical shell geometries were achieved by controlled particle-directed growth of Cu_2O shells on Au nanoplate, nanorod, and octahedron cores.[96] The Cu_2O shells were obtained by reacting a mixture of $CuCl_2$, sodium dodecyl sulfate surfactant, Au particles, basic aqueous solution. The Au particles located at the center of the hybrids and six {100}-faceted cuboctahedral Cu_2O shell attached on the Au octahedral core and the growth of the shell was precisely guided by the Au core shape. The electronic properties of the Cu_2O shells can be modified by inclusion of the Au cores, thus electrical conductivity of the Au–Cu_2O nanocubes is much better than that of Cu_2O particles.

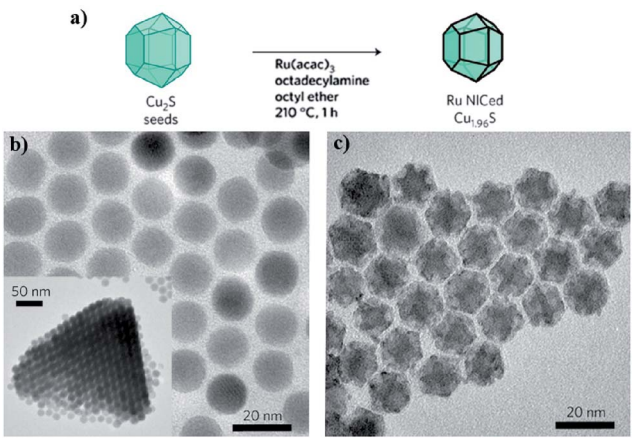

Fig. 7 Hybrid nanoscale inorganic cages. (a) Schematic illustration of the synthesis of cage-shaped nanohybrids. (b) TEM images of Cu_2S seeds, inset showing a 3-D superstructure from individual particle assemblies. (c) TEM image of Ru-NICed $Cu_{1.96}S$ particles. Reproduced with permission from ref. 84. Copyright 2010 Nature Publishing Group.

Thermal decomposition of the single component precursor of iron(III) oleate complexes in a sodium oleate–oleic acid–eicosane mixture under argon at 350 °C afforded biphasic core–shell $Fe_{1-x}O|Fe_{3-\delta}O_4$ nanocubes with rock salt–spinel interface (Fig. 8).[97] The core–shell structures formed could result in the release of CO during thermolysis that participates in the reduction of iron(II) to give $Fe_{1-x}O$ core and $Fe_{3-\delta}O_4$ shell with a thickness of ~5 nm. Oxidation of the core–shell structures by heating the colloidal dispersion under bubbling air resulted in the elimination of the interfacial strain of the $Fe_{1-x}O$ core, but the antiphase boundaries in the single-phase Fe_3O_4 nanocubes remained. The iron oxide nanocubes exhibit anomalous magnetic properties correlated with defects in the antiphase boundaries. Chen *et al.*[98] synthesized Au-peapodded Ga_2O_3 by thermal annealing of Au–Ga_2O_3 core–shell nanowires at high temperature. The size and shape of these nanohybrids can be manipulated by changing the annealing time and forming a gas. Cheng *et al.*[99] synthesized SnO_2 backbone-ZnO branch nanoarchitectures through epitaxial growth of ZnO rods on side facets of SnO_2 wires. The geometry of the ZnO backbones can be tailored both by changing the precursor concentration and by adding surfactants. The SnO_2/ZnO nanohybrids showed an enhanced near-band gap emission relative to the SnO_2 nanowires arising from the high-surface-area complex nanoarchitectures.

The plasmonic–magnetic nanohybrids were synthesized by incorporating magnetic (Co, Ni) heterometals into Au particles. A one-pot route to Au-based magnetic hybrids of Au–Co core–shell and Au–Ni spindly structures were developed by Wang *et al.*[100] The nanohybrids were obtained by solvolysis of $HAuCl_4$ and metal nitrate ($Co(NO_3)_2$ and $Ni(NO_3)_2$) as starting materials and octadecylamine as surfactant and reaction solvent. The Au–Co core–shells have a lattice spacing of 0.235 nm for the core and of 0.205 nm for the shell corresponding to cubic Au{111} and cubic Co{111} facets. The Au–Ni spindly nanostructures have lattice fringes with interplanar distances of 0.203 nm in both their tip and tail. Mazumder *et al.*[101] synthesized Pd/FePt core–shells by decorating FePt precursors on Pd seeds. Uniform coating and thickness of the FePt shells on the Pd seeds can be controlled by changing the ratio of Fe, Pt precursors, and Pd seed. Zeng *et al.*[102] synthesized bimagnetic $Fe_{58}Pt_{42}$–Fe_3O_4 core–shells from coating $Fe_{58}Pt_{42}$ core with Fe_3O_4 shell that occurred at high temperature. Magnetic shell thickness-dependent properties of these structures were found due to an exchange coupling between core and shell. A two-step procedure was reported by Ma *et al.*[103] on the synthesis of Au–Ag core–shell nanocubes with high yield of ~86–90%. CTAC-capped Au seeds were formed from the reaction solution containing $HAuCl_4$, CTAC, ascorbic acid, and Au particles. An aqueous $AgNO_3$ solution was added to the CTAC-capped Au seeds in the presence of ascorbic acid and CTAC to generate Au–Ag core–shells. The core–shell nanocubes were transformed into interior hollow nanocubes through a galvanic replacement process. The Ag shells were converted to porous Ag shells, while the Au cores were kept inside shells, and optical properties could be tuned by controlling the size and shape of the core–shells.

$CuInSe_2$/$CuInS_2$ core–shell nanobundles were synthesized by adding sulfur to a $CuInSe_2$ seed dispersion and polycrystalline $CuInS_2$ nanocable shells appeared of greater thickness with an increase in S/Se molar ratio.[105] The small radius of copper ions allowed a fast outward diffusion from interior particle surface to react with sulfur elements and indium ions, resulting in the formation of the $CuInS_2$ shells. Lee *et al.*[106] synthesized PbSe/CdSe/CdS hybrids with two distinct geometries of core–shell-shells and tetrapods and demonstrated the efficient emission in an infrared regime with exceptionally long lifetime decays. Fig. 9 shows a multi-step procedure reported by Liu *et al.*,[104] who synthesized Au/SiO_2/CdSe hybrids constituted of an Au core overcoated with SiO_2 shell with a dense monolayer of CdSe quantum dots. The products obtained involved the synthesis of Au particles, gold-particle surface activation, silica-shell deposition, modification of the silica surfaces with $-NH_2$ groups, and

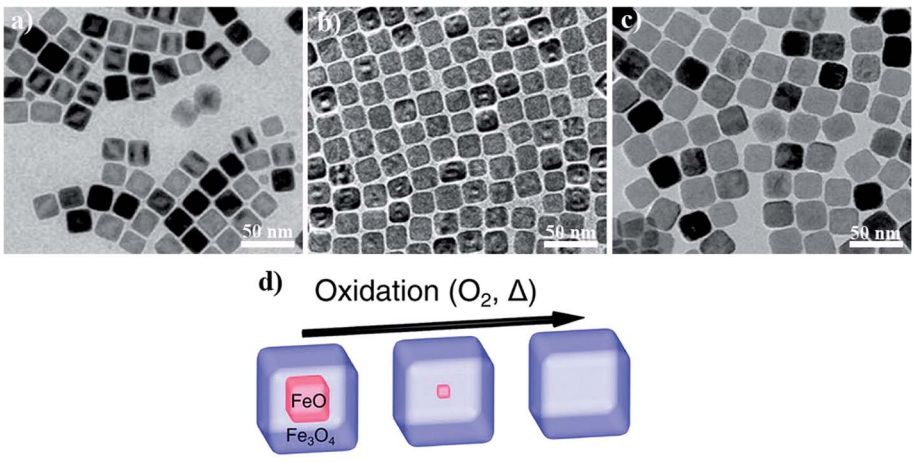

Fig. 8 Conversion of $Fe_{1-x}O$–$Fe_{3-\delta}O_4$ core–shells to single-phase Fe_3O_4 nanocubes. TEM images of (a) $Fe_{1-x}O|Fe_{3-\delta}O_4$ core–shells from thermolysis of iron(III) oleate complexes in a sodium oleate–oleic acid–eicosane mixture, which were oxidized to form nanocubes with defect structure after (b) 30 min and (c) 120 min. (d) Schematic illustration of the gradual elimination of the core of the $Fe_{1-x}O$–$Fe_{3-\delta}O_4$ hybrids during oxidation. Reproduced with permission from ref. 97. Copyright 2013 American Chemical Society.

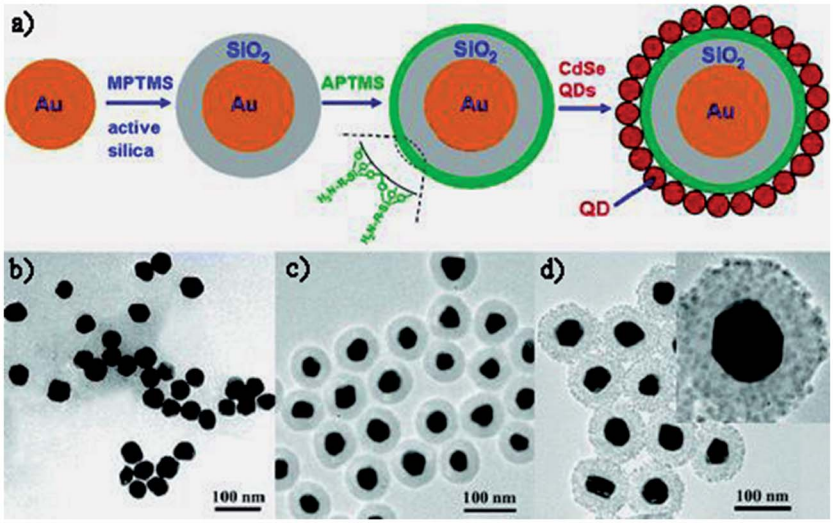

Fig. 9 Gold–silica–quantum dot nanohybrids. (a) Schematic illustration of multi-step synthesis of Au–SiO_2–CdSe hybrids, (b) TEM images of synthesized Au cores, (c) gold–silica core–shells, and (d) Au–SiO_2–CdSe hybrids, inset showing a single Au–SiO_2–CdSe hybrid particle. Reproduced with permission from ref. 104. Copyright 2006 American Chemical Society.

assembly of CdSe quantum dots on the particle surfaces. In order to obtain surface activation of gold particles, (3-mercaptopropyl)-trimethoxysilane was found to be better than (3-aminopropyl)-trimethoxysilane because of the stronger binding of –SH groups to the Au particle surfaces. The hybrid structures were used to perform quantitative analysis of the effect of the metal clusters on the quantum dot luminescence intensity.

The Janus nanoparticles with dumbbell and core–shell geometries prepared by UV light-induced growth and chemical deposition/coating offer a great opportunity for transferring their unique properties into modern practical applications of nanotechnology. The conjugation of the hybrid materials with biomolecules can produce organic–inorganic bioconjugates with emerging properties for imaging-guided therapy in biomedicine as presented in Section 5.1.

4.2. DNA-functionalized plasmonic structures

DNA-guided assembly of the nanoparticles represents an active research effort in DNA nanotechnology. The influences of the sequence and structure of the DNA on the deposition of the metal particles onto the oligonucleotide strands were reported.[107] Three-ring catenane nanostructures with plasmonic coupling and surface-enhanced fluorescence features can be obtained by functionalization of DNA rings with gold clusters.[108] Stable silver particle-attached DNA structures formed by using cyclic disulfide-modified DNA to protect the oxidation of the silver particle surface.[109] The immobilization of CdSe quantum dots onto thiol-modified DNA became more easily for the surface passivation of the quantum dots with 3-mercaptopropionic acid capping agent.[110] Employing copper-catalyzed alkyne–azide reaction allowed iron oxide particles attached to DNA through hybridization between alkyne groups of DNA and azide-modified particles.[111] Thiolated DNA functionalization onto the gold particles without requiring the capping agents to stabilize the particles produced gold–DNA nanohybrids.[112] The addition of polyethylene glycol to the reaction solution allowed the authors to increase the thiolated DNA loading within a shorter time than the previous method.[113]

The choice of the appropriate DNA ligands was achieved to form disordered gold/DNA amorphous structures that can be dynamically converted to highly ordered structures by annealing treatment. The number and interspacing of the DNA strands hybridized with the gold particles were effectively conducted using polyadenine as a diblock oligonucleotide.[115] Fig. 10a shows the formation of monothiol DNA immobilized onto gold cluster assemblies by taking advantage of balancing the cross-linking capability of dithiothreitol (DTT).[114] The use of DTT and monothiolated DNA allowed to control the size of the gold clusters attached onto DNA by changing the DTT and DNA ratio in the preparation.[108] In an interesting report by Li *et al.*,[116] the linear assembly of biotin-functionalized DNA triple template with streptavidin-functionalized gold particles through biotin–streptavidin interaction generated DNA-templated streptavidin–nanogold arrays. Sleiman *et al.*[117] achieved the encapsulation of gold particles into DNA nanotubes to form peapod-shaped particle chains with gold particles. Fig. 10b shows pyramid-shaped nanostructures of plasmonic and fluorescent assemblies made by self-organization from four different single strands of DNA building blocks.[52] More importantly, Macfarlane *et al.*[118] showed general rules for co-assembly of DNA-conjugated gold particles with DNA linker strands to construct organized DNA–gold superlattices.

The self-organization of the gold particles with either multihelix DNA bundles or 2-D DNA tiles upon thermal evaporation to fabricate 3-D tubular structures was reported by Mao *et al.*[119] Fig. 11 shows a big step forward made by Yan *et al.*,[25] who synthesized nanotubular structures with different 3-D architectures, such as stacked rings, single spirals, double spirals, and nested spirals, by attaching single-stranded DNA to gold

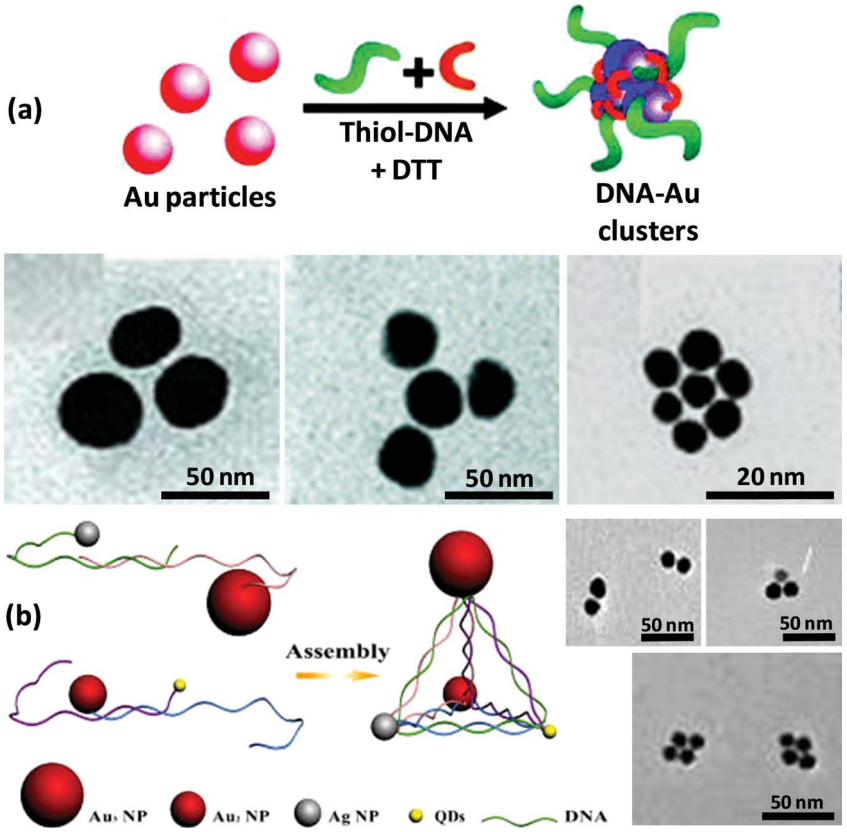

Fig. 10 Metal cluster-functionalized DNA conjugates synthesized *via* self-assembly. (a) Schematic illustration of DNA–gold conjugate synthesis. TEM images of DNA–Au particles with different size and shape conjugates. Reproduced with permission from ref. 114. Copyright 2006 American Chemical Society. (b) TEM images of assembled chiral pyramids made from the different particles of Au, Ag, and quantum dot. Reproduced with permission from ref. 52. Copyright 2012 American Chemical Society.

particles *via* self-assembly. Wei *et al.*[120] demonstrated chiral plasmons of assembled gold nanorod dimers with a twisting structure obtained by hybridization of chiral DNA bridges. Kiehl *et al.*[121] used prepared 2-D DNA scaffolds on the particle surface to assemble gold–DNA nanoarrays through complementary base pairing. Seeman *et al.*[122] synthesized 2-D gold particle assemblies templated by double DNA crossover triangles. Cheng *et al.*[123] prepared freestanding monolayered gold–DNA superlattice sheets by a microhole-confined dewetting process. Inter-particle spacing among gold particles and functional properties can be rationally controlled by adjusting DNA length. Yan *et al.*[124] modified this method to prepare gold particle-embedded 2-D DNA suprastructures with a sheet shape from the hybridization of the gold particles with DNA tiles. The authors prepared 2-D DNA nanogrids with ordered sticky strands to hybridize gold–DNA hybrids to form periodic square-like gold nanoarrays. Later, the authors used lipoic acid-modified gold–DNA hybrids with strong bivalent thiol–gold bonding for the assembly of DNA tiles decorated with a discrete number of the gold particles at the desired positions.[125]

Although the synthetic routes of the DNA-oriented plasmonic nanostructures are mostly available to date, however comparative studies on the fundamental properties and their structural simulations are necessary. Such materials derived from the DNA assembly offer access to a new model in the

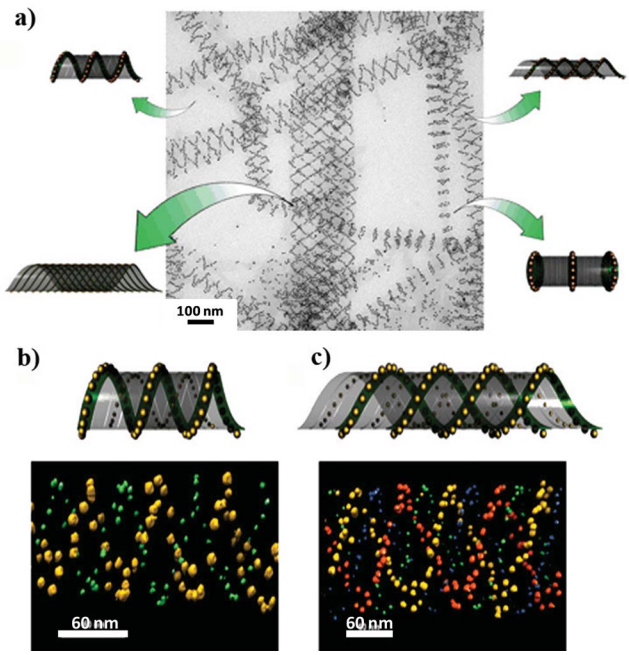

Fig. 11 Self-organization of DNA tubules through integration of Au particles. (a) TEM image of tubular structures carrying 5 nm Au particle-assembled DNA tile template. Tubes formed with (b) 5 nm and (c) 10 nm Au particles placed on the opposite surfaces of DNA arrays. Reproduced with permission from ref. 25. Copyright 2009 AAAS Science.

design of the promising biosensing devices as presented in section 5.2.

4.3. Photonic nanocrystal superlattices

Silica photonic crystals are synthesized by self-assembling monodisperse silica spheres into a crystalline lattice, giving structures akin to opals, since the Stöber report on the controlled growth of uniform, monodisperse silica microspheres in 1968.[126] Photonic opal structures exhibit strong optical confinement of light to a very small volume to induce brilliant structural colors.[39,40] The photonic structures offer the possibility to manipulate light by tuning stop-band position of the photonic structure in the visible region. Tunable lighting of the photonic structure has significantly enhanced sensing performance. Therefore, photonic sensors have been the subject of intensive research over the last decade especially for detection of a wide variety of biological and chemical substances.

This self-organized route has been extended to photonic nanostructured materials. Recent reports indicated that colloidal uniform nanoparticles can act as building blocks to self-assemble into a periodically photonic structure. In an another technique, as shown in Fig. 12, magnetically photonic nanocrystal arrays dispersed in a desired solution is prepared by applying an external magnetic field.[74] This robust procedure allows the construction of tunable photonic superlattices from the self-assembly of highly charged superparamagnetic Fe_3O_4 colloidal clusters in aqueous and non-aqueous solutions. The Fe_3O_4 clusters were prepared by hydrolyzing $FeCl_3$ in a basic diethylene glycol solution containing polyacrylic acid as the capping agent. The subsequent coating of polyacrylate with the nanocrystal clusters was carried out to form highly negative charged particle surfaces rendering them soluble in water. The polyacrylate-capped Fe_3O_4 nanoclusters were coated with a silica layer to form positively charged SiO_2@Fe_3O_4 core–shells dispersed in a non-aqueous solution.[127] Then, these building blocks aggregated uniformly into ordered linear chains along the direction of the external magnetic field, where the magnetic attractive force results to bring the particles together. Long-range 3-D order of the formed colloidal crystals is a balanced result of the magnetic force and interparticle electrostatic repulsive force. The self-assembly process still retains the superparamagnetic property of the individual Fe_3O_4 clusters

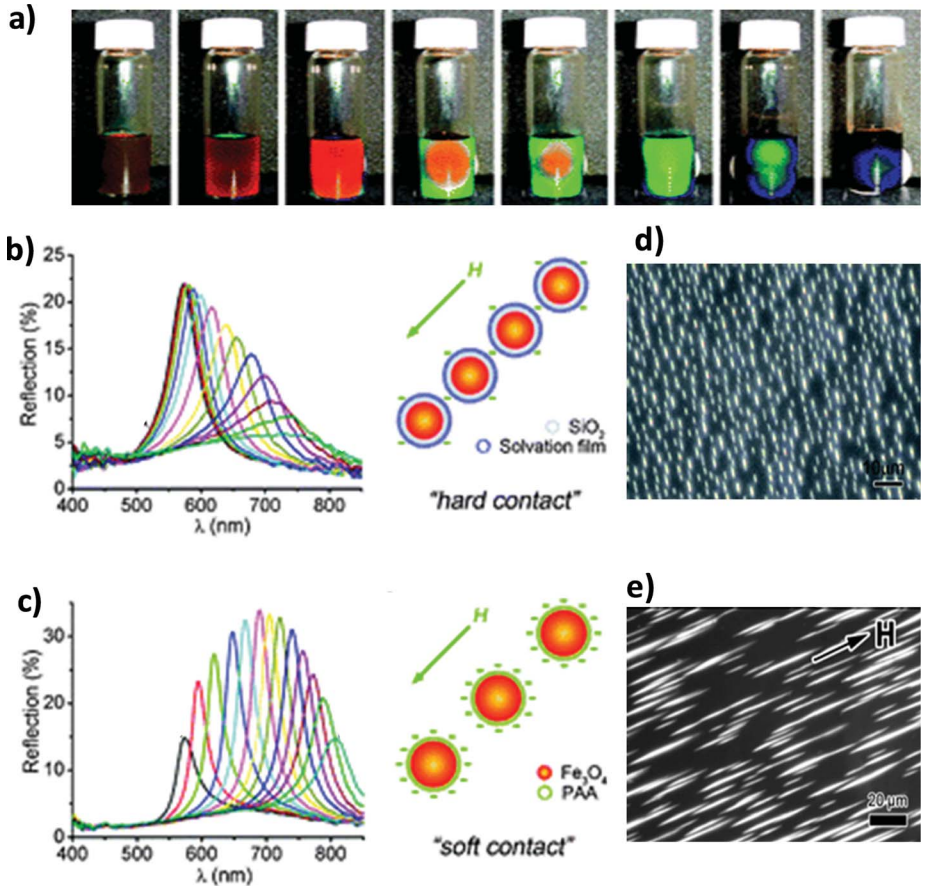

Fig. 12 Magnetically photonic nanocrystal assembles dispersed in water. (a) Photograph of the superlattice colloids formed in response to the variance of the strength of the external magnetic field. Dependence of the reflection spectra at normal incidence of (b) polyacrylate-capped Fe_3O_4 nanoarrays and (c) silica-coated polyacrylate-capped Fe_3O_4 nanoarrays on the distance of the sample from the magnet. Optical microscopy images of (d) the polyacrylate-capped Fe_3O_4 nanoarrays and (e) the silica-coated polyacrylate-capped Fe_3O_4 nanoarrays under an external magnetic field. Reproduced with permission from ref. 75. Copyright 2008 Wiley-VCH. Reproduced with permission from ref. 127. Copyright 2012 American Chemical Society.

alongside an increase in the saturation magnetization arising from the large, secondary structures. Upon application of a magnetic field, most particle chains align parallel to the external magnetic field as straight strings with periodic lattice spacing, thus showing monochromatic colors when the periodicity of the assembled photonic structures closely matches the wavelength of the incident light. The photonic Fe_3O_4 nanoarray colloids can be used as sensitive optical sensors in response to external magnetic fields. The periodicity of the assemblies can be controlled by manipulating the strength of the external magnetic field, thus tuning the diffraction wavelength throughout the entire visible spectrum. The particle size of the clusters and ionic strength of the solution are sensitive to tuning the optical responses. The photonic crystals of the large clusters diffracted red light in a weak magnetic field, while a blue color was observed in more ordered structures assembled from the clusters.

Gravitational sedimentation technique was applied to assemble monodisperse Ag particle colloids into conjectured densest packing arrangements with large domains.[128] The silver particles with controlled shapes were prepared by polyol reaction using polyvinylpyrrolidone (PVP) stabilizer. *N*,*N*-Dimethylformamide dispersion of PVP-stabilized silver particles was loaded into a reservoir containing polydimethylsiloxane (PDMS) and allowed the particles to fill into the channels. The dense supercrystals were formed by tilting the reservoir to gradually sediment the particles at the bottom. The dense supercrystal assemblies reflected light to induce the physical colors observed under crossed polarizers demonstrating the long-range order of the superlattices. The gravitational sedimentation gave the superstructures with organization more periodicity than that prepared from drying-mediated assembly of the silver particle dispersion on the substrate owing to the severity of solvation forces.

The construction of the photonic nanomaterials from the uniform building blocks can create new physical features different from the dispersed constituents or disordered counterparts, while retaining the individual properties. The nanocrystal superlattice films are emerging as an important class of promising nanomaterials for the design of opto-electronic devices. The optical properties of such materials have to offer for photonic applications are highlighted in Section 5.3.

5. Innovative applications

5.1. Cancer therapeutics and diagnostics

The biomolecule-conjugated Janus nanoparticles have been considered as potential magnetic resonance imaging (MRI) contrast and anticancer agents arising from biocompatibility in human organisms.[129] Such materials are used extensively for integrated magnetic and optical applications in biomedicine unavailable in conventional single nanocomponents. The dumbbell and core–shell Janus particles can offer two functional surfaces for attachment of the biomolecules of proteins, antibodies, and therapeutic molecules, making them especially attractive as multifunctional probes for drug delivery and imaging-guided therapy. MRI is presently one of the most powerful diagnostic tools in biomedicine for imaging the central nervous system and detecting cancerous tumors.[130] Among them, paramagnetic gadolinium chelate complexes (*e.g.*, Gd–Gadopentetic acid) are widely used as MRI contrast agents.[131] Recent efforts in the development of nanocomposites by combination of different components produce new multifunctional materials, *e.g.*, plasmonic–magnetic nanohybrid MRI contrast agents show improved contrasting abilities and have extra functions.[132]

Surface-modification methods have been devoted to developing the nanohybrid-based MRI contrast agents and endow compatibility in the biological environment. Generally, there are two routes to encapsulation with biocompatible shells and ligand exchange with water-soluble ligands. For example, hollow SiO_2@FeOOH nanocapsules used for MRI contrast agents were prepared by coating FeOOH with a silica layer.[133] In other works, oleic acid–oleylamine-capped Au–Fe_3O_4 dumbbells functionalized with dopamine and thiol groups were used for dual MR and optical imaging. Epidermal growth factor receptor (EGFR) is an antibody to target A431 cells, thus imaging EGFR over-expressed cells and tissues can potentially be used for early diagnostics and therapies of lung and breast cancers. Bioconjugation of the Au–Fe_3O_4 dumbbells prepared by using EGFR to link with PEG by (1-ethyl-3-(3-dimethyllaminopropyl) carbodiimide/*N*-hydroxysuccinimide) on the particle surface afforded efficient cancer-targeted MR imaging agents.[134,135]

The targeted diagnosis, isolation, and photothermal destruction of human breast cancer cells based on S6 aptamer-conjugated Au–Fe_3O_4 nanohybrids were reported by Fan *et al.*[136] The Au–Fe_3O_4 materials exhibit bifunctional properties, in which the plasmonic shell functions as both a photothermal agent and a nanoplatform and, simultaneously the magnetic core is effective for cell isolation. The bioconjugated Au–Fe_3O_4 particles were applied for targeted imaging and magnetic separation of a specific cell from a mixture of different cancer cells based on selective interaction between the S6 aptamer and the cancer cell. The imaging analyses of photothermal destruction indicated selective irreparable cellular damage to the cancer cells resulting from the absorption of 670 nm NIR irradiation of the nanohybrids. MRI contrast agent and carrier in the anticancer drug delivery of core–shell structured hollow mesoporous nanocapsules of $Fe_2O_3/SiO_2/mSiO_2$ and $Au/SiO_2/mSiO_2$ were reported by Chen *et al.*[94] The mesoporous nanocapsules show good dispersion in the cytoplasm and no nanocarriers were found in the nucleus, demonstrating the efficiency in fluorescent cell imaging and anticancer drugs delivery into the cancer cells. Vesicles formed from existing nanocapsules near cell membranes can be observed by fluorescent microscopy. The nanocapsules were processed in endosomes and lysosomes and eventually released into the cytoplasm after absorbing cancer cells through endocytosis. The excellent biocompatibility of the mesoporous Fe_3O_4/SiO_2 nanocapsules makes them function as efficient carriers in drug delivery and as MRI contrasting agents.

The studies of cellular internalization, toxicity, and innate immune response of SiO_2/TiO_2 hollows with particle diameters of 25, 50, 75, 100, and 125 nm in human breast cancer and

mouse alveolar macrophage cells were reported by Jang *et al.*[138] The particle size and surface functionalization affected the response of the SiO_2/TiO_2 hollows. A highly uptake ratio of 50 nm and 70 nm SiO_2/TiO_2 hollows into SK-BR-3 and J774A live cells was observed by microscopic imaging. Well-dispersed and stabilized micellar quantum dot hybrids came from strong interaction of the hydrophobic chains of PEG–phospholipids with the hydrophobic chains attaching on the particle surface. Simultaneous dual-mode diagnosis and therapy with the hybrids were applied for more effective early detection and treatment of various types of the cancers. Ying *et al.*[139] reported that biocompatible silica-coated quantum dots or magnetic particles through reverse microemulsion can effectively target the cell membranes of HepG2 human liver cancer cells, NIH-3T3 mouse fibroblast cells, and 4T1 mouse breast cancer cells.

Bioconjugation of the targeting ligand F3 peptide with magnetic fluorescent nanocomposites functionalized with PEG-modified phospholipid makes these multifunctional nanomaterials function in drug delivery and enables dual-mode magnetofluorescent imaging of cells (Fig. 13).[137] Triantennary dendritic galactoside-linked ZnS/CdSe nanohybrids act as hydrophilic, fluorescent, and multivalent probes for detecting metastatic lung cancer cells.[141] The water-soluble nanohybrids were selectively takenup by lung cancer cells enriched with membrane-bound protein receptors. The nanohybrids entered cancer cell cytosol rather than onto the cellular surface. The results suggested strong interactions between poly-hydroxylended nanohybrids in the membrane composition and the cancer cells. Mesoporous dye-doped SiO_2 particles decorated with multiple magnetite particles for simultaneously enhanced magnetic resonance imaging, fluorescence imaging, and drug delivery.[142] In an another report, peptide-conjugated CdS:Mn/ZnS fluorescent–magnetic core–shells possessing fluorescence, radio-opacity, and paramagnetic properties were used to label and visualise brain tissue without manipulating the blood–brain-barrier. Fluorescent visualisation of whole rat brain was achieved using a low-power handheld UV lamp, indicating that these materials could potentially be applied for sensitive multimodal detection.[143]

Lanthanide-based upconverting nanoparticles are capable of converting near-infrared excitation to tunable luminescence from the UV to the NIR range.[144] These materials are attractive for therapeutic imaging arising from their improved properties of exceptional photostability, deep tissue penetration and suppression of autofluorescence, and low toxicity. There has been investigated the bioconjugated synthesis and design of these promising nanomaterials for improving current biomedical barriers. Fig. 14 shows a synthetic procedure of

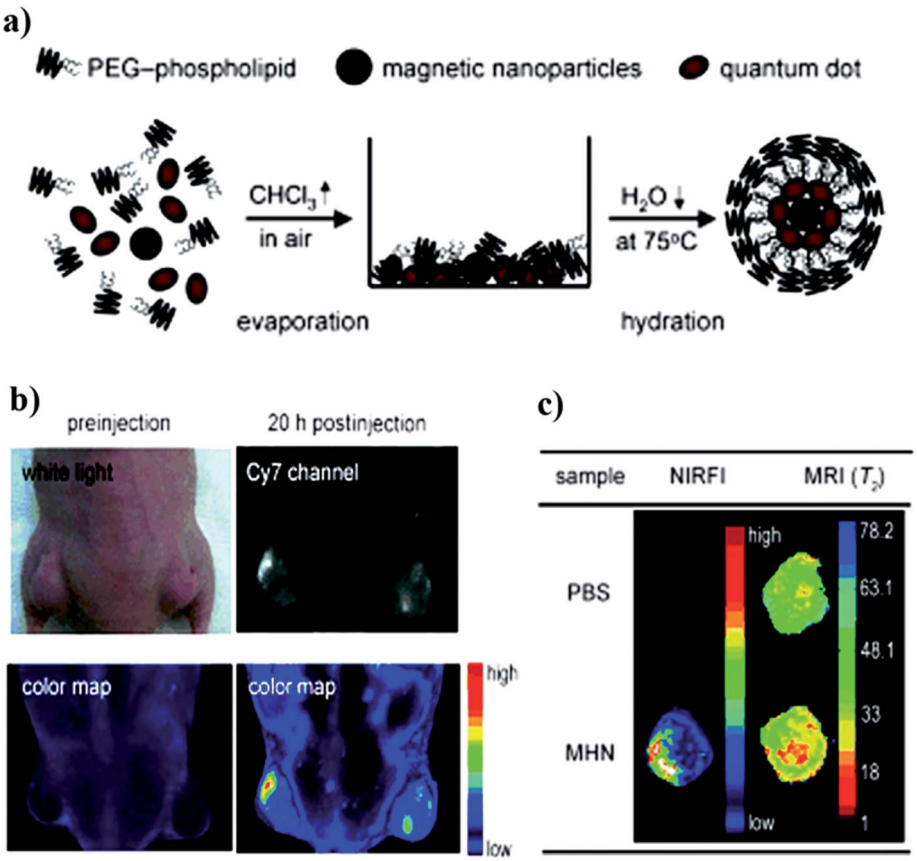

Fig. 13 Magnetic semiconducting nanohybrids for simultaneously magnetofluorescent imaging and drug delivery. (a) Synthetic procedure of micellar nanohybrids encapsulated in PEG-modified phopholipid micelles. (b) NIR fluorescence images showing passive accumulation of the nanohybrids containing magnetic and fluorescent particles in a mouse with MDA-MB-435 tumors. (c) Image table describing results of multimodal imaging of tumor cells harvested from the mouse in (b). Reproduced with permission from ref. 137. Copyright 2008 Wiley-VCH.

DNA-functionalized $NaMF_4$:Yb^{3+}/Ln^{3+} (UC) particles and Au-deposited UC hybrids. These materials were used as versatile agents for targeted imaging of the cancer cells based on aptamer–UC bioconjugates.[140] The bioconjugation of 26-mer DNA aptamer AS1411 with UC particles was achieved to produce Apta–UC conjugates. Subsequent analyses of the incubation of the Apta–UC materials in MCF-7 cells by observing confocal fluorescence and bright-field images indicated that the strong upconverting fluorescence is mainly on the surface of the MCF-7 cells. The aptamer-mediated accumulation of the Apta–UC particles can be readily taken up by cells and visualized under NIR light excitation with high photostability.

A clever combination of up-converting luminescence with magnetic properties into a multifunctional mesoporous Fe_3O_4@SiO_2@Y_2O_3/Yb,Er nanomaterial was reported by Zhang *et al.*[145] The magnetic upconverting fluoride nanorattles were conjugated with the antitumor drug doxorubicin for drug delivery. Through *in vitro* experiments in mice cells, the authors demonstrated that the material emits visible luminescence upon NIR excitation and can be directed by an external magnetic field to a specific target, making them an attractive system for targeted chemotherapy. Mesoporous silica-coated $NaYF_4$:Yb,Er upconverting fluorescent particles (UCs) functioning as a remote-controlled nanotransducer for photodynamic therapy were reported by Zhang *et al.*[21] The particle matrix can efficiently upconvert the energy penetrating near-infrared light to visible light and transfer it to the encapsulated photosensitizers. The UC materials showed a spectral overlap between emitted visible light and maximum absorption wavelengths of the photosensitizers to generate cytotoxic singlet oxygen in water. The inhibition of tumor cell growth in the mice resulted from releasing singlet oxygen from UCs, even at low 980 nm laser power. This enabled selective fluorescent labelling, imaging and potentially sorting of the cells opening new prospects in cancer diagnostics and therapy.

Although such nanocomposites have been used for *in vitro* magnetic cell separation and *in vitro* cell targeting, *in vivo* studies, in particular for cancer imaging and therapy, have still presented major challenges for transferring into clinical practices.[146] Integrated collaboration of materials scientists with biologists and clinicians to become interdisciplinary teams should be established to systematically demonstrate and evaluate specific properties of the preformed hybrid nanomaterials, such as long-term toxicity, pharmacokinetics, and any disinfection byproduct effects.

5.2. DNA-functionalized plasmonic probes

Simultaneous integration of plasmonic property and circular dichroism signals derived from chiral dipolar coupling of the

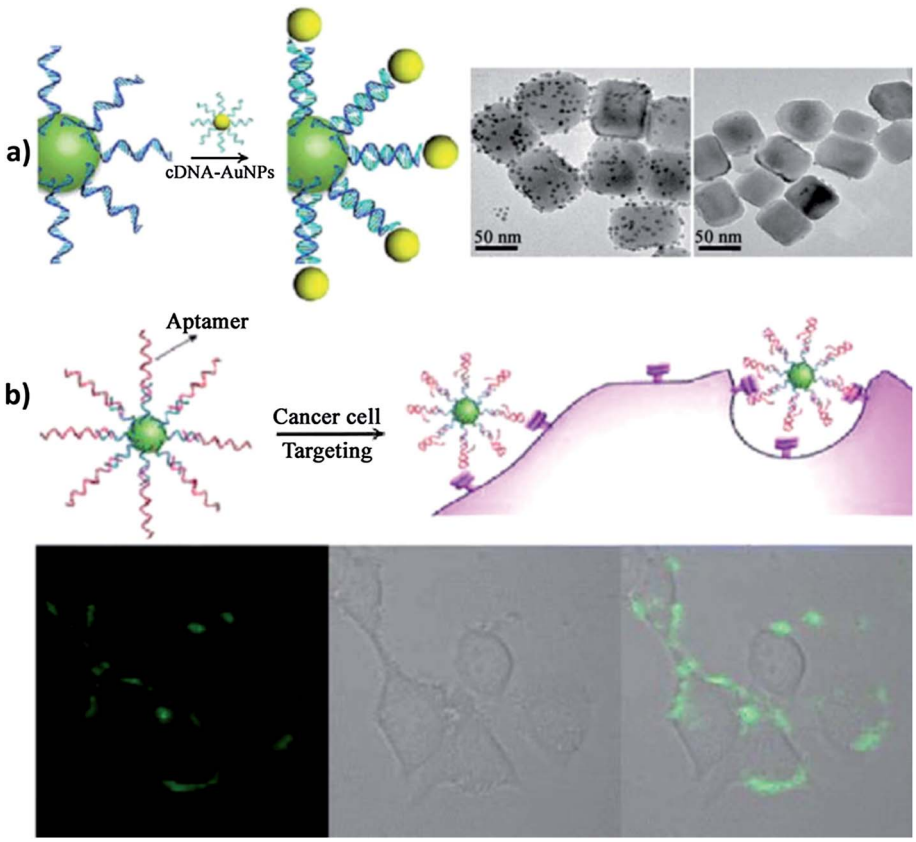

Fig. 14 DNA-functionalized upconverting particles as biocompatible agents for DNA delivery and imaging. (a) DNA-directed assembly of $NaMF_4$:Yb^{3+}/Ln^{3+} (UC) particles and Au–UC hybrids and their corresponding TEM images. (b) Schematic illustration and targeted imaging of the cancer cells with aptamer–upconversion bioconjugates. Confocal microscopy images of MCF-7 cells treated with Apta–UC particles. Reproduced with permission from ref. 140. Copyright 2013 American Chemical Society.

surface plasmon resource into a metal-functionalized DNA nanostructure is ideal for optical biosensing applications.[8] Incorporation of functional plasmonic dopants into helical DNA structures can advance their optical responses, useful for the design of biosensing devices responsive to external environments. The plasmonic metal (*e.g.*, Au and Ag) particles are ideal SERS probes with their tunable optical properties arising from quantum confinement effects.[2] Significantly, diagnostic application of DNA–metal clusters is demonstrated by a sensitive and selective colorimetric assay, in which target sequences are detected based upon unique properties of the assembled clusters. Coupling of opto-electronic properties of the DNA structures with plasmonic particles can provide new materials with potential uses in the biosensing field.[7] Plasmon–DNA based platforms have found applications in the development of biosensors, therapeutics, and diagnostic tools in the biomedical field.[147,148] In this section, we present recent progress by materials researchers in the use of the plasmonic metal-functionalized DNA nanostructures with hierarchical geometries as highly selective SERS bioprobes.

To enable these applications, a crucial step is to attach DNA on the solid particles. The metal particles have been the most studied subjects in this field because of the well-established method for DNA attachment based on thiol adsorption on the particle surface. Heteropentamer clusters with remarkably magnetic properties made up of a smaller Au sphere surrounded by a ring of four larger spheres were generated from the assembly of gold–DNA hybrids.[149] Therein, DNA is not only crucial for the cluster assembly, but also functions as an insulator spacer between conductive particles. Further, in a quest to make highly sensitive and signal reproducible SERS probes with high stability, Nam *et al.*[150] reported the synthesis of Au bridged nanogap particles with an interior gap size of 1 nm. Interestingly, DNA plays important roles in sparse nucleation sites of the Au particles on the Au–DNA surface and lateral growth of the Au shell and the formation of a 1 nm interior gap inside particles, which is unusual for shell growth on a core surface.[151] During the synthesis, the position and number of Raman dyes can be readily controlled and the dyes can be precisely located in a 1 nm interior gap for generating the SERS enhancement factors with a narrow distribution. Azobenzene-modified oligonucleotide-functionalized Au particles showed a reversible photo-switchable assembly.[152] Irradiation of UV light caused *trans–cis* isomerization of azobenzene, destabilizing the DNA duplex, resulting in the dissociation of the particle assemblies, which can be reassembled by illuminating them with blue light. Stable gold–silver core–shell structures were synthesized from the Au–DNA particles to generate DNA-embedded Au–Ag core–shell particles by the silver staining method, where the silver shell thickness is controllable based on the amount of silver staining solution used in the synthesis.[151]

The anisotropic structures of metal particles (Au rod and prism shapes) were often prepared using seed-mediated growth in the presence of CTAB capping agent.[153] The Au particles with anisotropic shapes have positively charged surfaces originating from capping of CTAB ligands on the particle surfaces, which electrostatically interact with oppositely charged DNA. Thus, the functionalization mechanism of the anisotropic metal particles on DNA is slightly different from the isotropic metal particles. To address this issue, the CTAB-capped Au particles are washed several times to remove partial CTAB ligands and then functionalized with thiol-modified DNA. Overcoming this problem allows the exploitation of the oriented assembly of anisotropic metal particles (*e.g.* Au rods) to generate well-defined complex superstructures with new collective properties. Mann *et al.*[154] achieved an unprecedented hybridization of 3-D DNA bundles with Au nanorods through DNA complementary binding to yield Au–DNA parallel stacks. The discovery of using the DNA ligand with helical structure resulted in producing helical Au–DNA hybrid replicas. The Au nanorods were decorated on the DNA helix, which was characterized by reversible plasmonic circular dichroism (CD) responses. The simultaneous response of the plasmonic Au rods through CD and UV-Vis signals proved to be of great significance for the design of sensitive biosensors for DNA detection.[155] The anisotropic metal particles have higher interparticle surface contact than isotropic particles, which gave a higher hybridization efficiency for the same amount of DNA loading employed. The oriented attachment of the anisotropic particles with DNA strands often occurred at parallel face-to-face interactions between particles to maximize their surface contact. Fig. 15 shows Yan *et al.*'s work on the DNA-driven self-organization from individual building blocks of Au, Ag, quantum dots onto chiral particle pyramids with tunable chiral properties.[52] The CD spectra exhibit the tunable positions of the CD signals in a wide range of UV and visible wavelengths. These responsive chiral nanomaterials expect to open extensive opportunities for research and instill stronger confidence in the viability of chirality-based optical devices.

Size-dependent steric repulsion effects are proposed for the control of specific tube conformations. Triangular-shaped DNA origami structures are used as a template for the well-controlled assembly of Au–DNA nanohybrids, affording dimeric and trimeric structures with tunable inter-particle distance.[156] Ding *et al.*[157] utilized a similar triangular-shaped DNA origami structure having different sticky ends for the linear assembly of six differently sized Au–DNA nanohybrids. Each Au particle was bound to three sticky ends and the spacing between particles was controlled by the position of these sticky ends. Access to such discrete gold–silver assemblies with tunable interparticle distance is significant from the viewpoint of their applications in the field of plasmonics. For more practical applications of the template approach in electronics and photonics, DNA-origami structures were arranged on the binding sites generated through electron beam lithography on silica and diamond-like carbon substrates in controlled orientations and 5 nm gold particles were assembled on them.[158] Yan *et al.*[159] utilized triangular DNA origami structures to assemble gold rod dimers with various well-defined inter-rod angles and relative distances. Acuna *et al.*[160] reported that attaching a couple of gold particles to DNA origami structures leads to a fluorescence enhancement at docking sites of DNA-directed gold dimer assemblies. In an interesting example recently reported by Kuzyk *et al.*,[13] as seen in Fig. 16, Au–DNA nanohybrids were

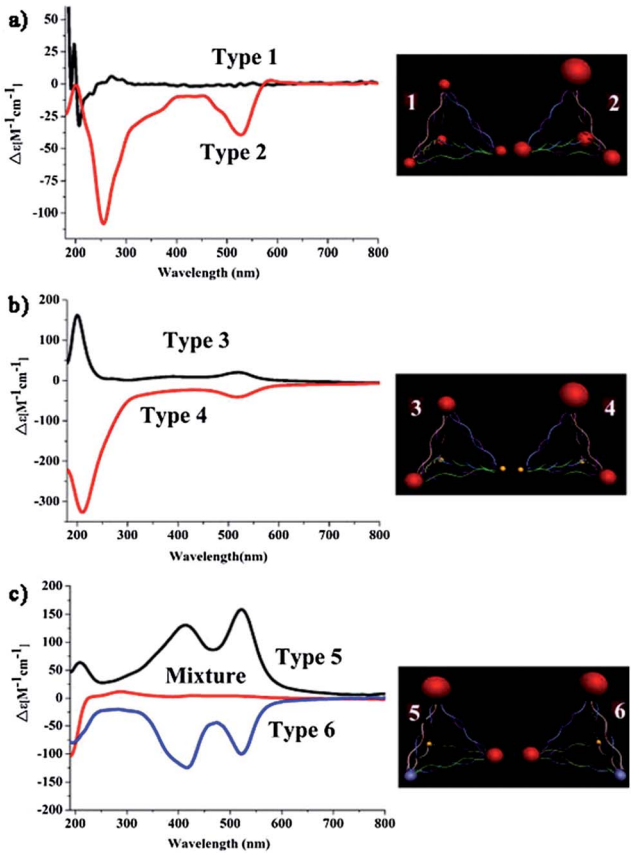

Fig. 15 Self-organization of chiral particle pyramids with tailored optical response. Circular dichroism spectra of self-organized pyramids made from (a) four Au_1 (type 1) and three Au_2 + Au_3 (type 2); (b) two Au_2 + two QDs (type 3), and Au_2 + Au_3 + two QDs (type 4); and (c) Au_2 + Au_3 + Ag + quantum dot as *S*- (type 5) and *R*-enantiomers (type 6). Reproduced with permission from ref. 52. Copyright 2013 American Chemical Society.

arranged in chiral helical arrangement on a long-range DNA scaffold *via* a DNA-origami approach. Such 3D chiral assemblies of Au particle exhibited CD responses in the visible region analogous to the chiral proteins and DNA showing the CD in ultraviolet and infrared regions. The left-handed and right-handed chiral assembled structures in solution exhibit the tunability of the CD peak over visible wavelengths that originate from collective plasmon–plasmon interactions of the particles positioned onto DNA helix templates.

Chiral DNA suprastructures are attractive natural templates for preparing solid-state materials as they have the possibility to transfer their chiral properties to solid replicas. Inventions of these unique properties of DNA for surface templation and supramolecular chemistry is of enormous scope to open effective paradigms for the design of DNA-based derivatives. The coupling of hierarchical DNA with desired plasmonic particles gives to rise highly selective features of the new materials in biodetection, which is key to obtaining reliable amplified signals. Although much effort has been made in the advancement of DNA production, the cost of commercial DNA products is very expensive, thus it is extremely difficult to largely synthesize these materials for widespread and practical applications. With the continuous improvement in biotechnology of DNA, materials scientists have anticipated that the production scale-up of the chiral helical assemblies of the plasmonic particles onto DNA templates over deposition control will be overcome in the near future to develop such free-standing materials. Going forward, the controlled templation of the helical DNA bundles with plasmonic particles could be highly beneficial for applications in electronics and photonics.

5.3. Superlattice optical responses

Photonic structures are an emerging class of optical materials. Of particular technological interest is the development of such materials with band-gap property in response to external stimuli for the fabrication of biochemical sensors, color paints and inks, reflective displays, and optical filters and switches.[39,161] Periodic nanocrystal arrays, which can be produced by assembling uniform particle colloids, are useful for making tunable photonic structures by means of applying an external stimuli.[36,38]

As opal structures, the assembled particle arrays have a periodic structure that can create a photonic band-gap by prohibiting propagation of a certain wavelength, thus typically generating structural colors.[40] The tunable photonic properties originating from modulating stop-band position of the assembled nanostructures can be employed by changing charge, the added electrolyte, and surface effect of the particle units. The photonic architectures can function as sensitive sensors because of the capability of tuning their optical properties by external stimuli. The formation of the pore space between assembled particles allows the stimuli-responsive components to be incorporated into the colloidal crystals by interacting building blocks, giving rise to tuning of their diffraction colors. In this section, we describe recent advances in integrated photonic patterns and sensors to be realized with low-cost processes and which are suitable for mass-scale production.

Responsive photonic crystals are appealing because their diffraction wavelengths and color emission can be controlled by external stimuli, for example, temperature or pressure, rather than modifying the material itself. This feature is well-suited to applications, such as color displays, biochemical sensors, security devices, and printing systems.[44] However, challenges, such as narrow tunability of the band gap, slow response to external stimuli, irreversibility, and difficult integration into existing photonic systems, affect the performance of some photonic crystals. To address these concerns, Yin *et al.*[74] first prepared highly charged, uniform superparamagnetic colloids and then self-assembled them into ordered nanoarrays. The colloidal assemblies are reversibly color-tunable across the entire visible spectrum under the influence of the external magnetic fields.

The use of the external magnetic field to guide the attachment of the uniform magnetic particle colloids into an ordered superstructure were reported for the first time by the Yin group.[74] The key point to the successful assembly of such magnetically responsive photonic nanocrystal structures is an established balance between repulsive and attractive interactions. The authors found that the assembled aqueous route under the

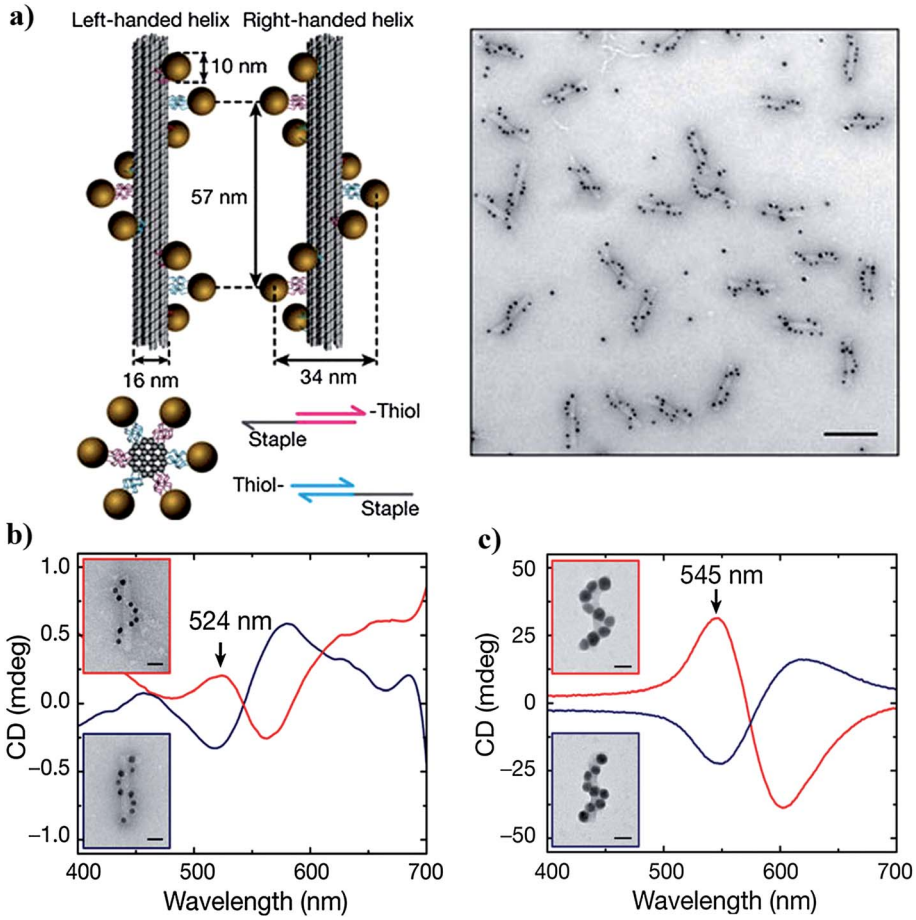

Fig. 16 DNA-based self-organization of chiral plasmonic nanostructures with tailored optical response. (a) Au–DNA particle assemblies composed of 10 nm Au particles attached in a helical arrangement to DNA helix bundle surface. TEM image of left-handed Au-assembled DNA nanohelices, scale bar = 100 nm. (b) Circular dichroism response of the nanohelices shifted to shorter wavelengths by growth of Ag shells onto 10 nm Au particles. (c) Circular dichroism response of the DNA-based assemblies with their signal strength originated from further growth of the metal particles with larger size on the nanohelices. Reproduced with permission from ref. 13. Copyright 2011 Nature Publishing Group.

assistance of the external magnetic field has been extended to nonpolar solutions.[75] The surface modification of the clusters with alkoxysilane layers formed a SiO_2@Fe_3O_4 core–shell structure.[127] The interparticle repulsion of these core–shell assemblies were well-dispersed in nonaqueous alkanol solutions including methanol, ethanol, ethylene glycol, and glycerol, resulting from the electrostatic and solvation forces. The optical properties of the core–shell assemblies in the non-aqueous solution resemble those of the photonic crystals dispersed in aqueous solution. The tunable monochromatic colors observed from the nanocolloids-dispersed solution are derived from the optical diffraction of the ordered core-shell assemblies in varying the external magnetic fields. The silica surface of the photonic crystals allowed the authors to incorporate them into a polydimethylsiloxane film in the form of liquid droplets. The flexible photonic solid patterns with tunable blue monochromatic colors represent a significant step forward for the potential use of these materials in display and sensing techniques with field-responsive optical properties (Fig. 17b).

Recently, the Yin group[165] discovered that polyacrylic acid-stabilized Fe_3O_4 nanocrystals with high surface charge and superior dispersibility in water make their aqueous dispersion as an ideal ferrofluidic media for orienting 185 nm-sized polystyrene beads in a magnetic hole assembly. Photonic structures with polystyrene 1-D and 3-D chain assemblies, which formed under corresponding weakly and strongly external magnetic fields were determined by interplaying magnetic dipole force and packing force. Thin liquid films were prepared by sandwiching the drops of mixed Fe_3O_4 clusters and polystyrene beads solution between two cover glasses. Upon application of the weak magnetic field, the tunable green-blue monochromatic spots of the films were observed under optical microscopy originating from the diffraction of the aligned polystyrene chains with periodically interparticle distances comparable to the wavelength of visible light. While the 3-D polystyrene photonic structures formed under a strongly magnetic field have a high reflectance in the visible range in response to the external magnetic field with varying strength and length of the time applied.

One interesting example of the assembly of the surface-modified Fe_3O_4 clusters into chain-like structures confined inside a microemulsion droplet was reported by the Yin group.[54]

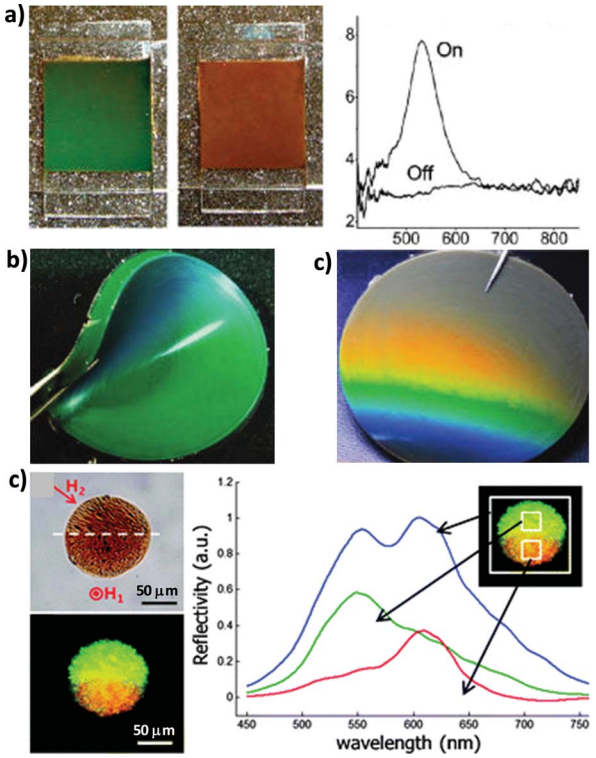

Fig. 17 Magnetically responsive photonic nanocrystal arrays. (a) Photographs of Fe_3O_4@SiO_2/PEGDA microspheres and their reflectance spectra showing diffraction peaks at the "on" stage and none at the "off" stage in response to heating–cooling and applied magnetic field. Reproduced with permission from ref. 54. Copyright 2009 American Chemical Society. (b) Photographs of a freestanding polydimethylsiloxane film displaying tunable iridescence in a nonuniform magnetic field. Reproduced with permission from ref. 15. Copyright 2012 American Chemical Society. (c) Reflective spectra of dual-colored photonic Janus balls of superparamagnetic nanoclusters/polydimethylsiloxane composites; inset showing their corresponding reflective image. Reproduced with permission from ref. 162. Copyright 2012 The Royal Society of Chemistry. (d) Iridescent pattern formed by assembling polystyrene beads on dumbbell-shaped nonmagnetic templates. Reproduced with permission from ref. 163. Copyright 2013 American Chemical Society. (e) Photograph of iridescent letters written on the display manually by using a small magnet as a pen. Reproduced with permission from ref. 164. Copyright 2013 The Royal Society of Chemistry.

In response to the application of the external magnetic field, the SiO_2-coated Fe_3O_4 particles assembled into ordered structures inside emulsion droplets. Polymerization of poly(ethyleneglycol) diacrylate (PEGDA) oligomers quickly occurred upon UV illumination to transform the emulsion droplets into solid polymer microspheres. The resin microspheres assembled with magnetic particles retained the diffractive colors resulting from fixing the periodic chains of the Fe_3O_4 particle assemblies inside a solid structure. The Fe_3O_4@SiO_2/PEGDA microspheres loaded in glass cells filled with poly(ethylene glycol) were demonstrated as switchable color display sensors by changing the sphere orientation. The matrix materials melted as heating the films to 46 °C allowed the display of the monochromatic colors by improving the aligned microspheres under magnetic field. The orientation of the microspheres in the matrix solidifies and was fixed as cooled to room temperature, which led to gradual tuning of the colors and reflectance absorbance. This photonic property can be switched "on" and "off" multiple times by means of heating and–cooling and applied magnetic field, respectively (Fig. 17a). In addition a combination of the external magnetic field with UV irradiation allowed to simultaneously assemble and polymerize both the magnetic clusters and UV-curable resin monomers into dual-colored photonic Janus balls with tunable photonic properties (Fig. 17c).[162]

The key of the external magnetic field-guided particle assemblies is to create magnetic micropatterns and electronic papers. Fig. 17d shows photonic patterns with iridescent colors obtained by immersing a nonmagnetic polyurethane polymer pattern in a magnetized ferrofluid upon modulating the locally external magnetic field around the pattern.[163] The magnetic interactions between nonmagnetic objects dispersed in the ferrofluid led to the assembly of these objects at positions defined by the polymer pattern template, providing photopatterns. Fig. 17e shows that 1-D nanochains assembled from periodically arranged superparamagnetic particles can be used as magnetically rewritable photonic ink of the basic color units to write on patterns.[164] The photonic pattern responses obtained behave like electronic papers displaying green iridescence, which can be magnetically switched "on" and "off" rapidly by tuning the direction of the external magnetic fields.

The superstructure materials derived from EISA of the monodisperse, uniform single and binary particles have found diverse applications. For example, Redl *et al.*[73] employed the drying of the alkane (hexane and pentane) dispersion of a variety of colloidal Fe_3O_4, FePt, PbTe, PbS nanocrystals on the different substrates (acetonitrile-coated teflon and SiO_2/Si wafer) to form superlattice films. The long-range order of the nanocrystal superlattice assemblies resulted to show a highly periodic stripe pattern observed under optical micrograph and iridescent colors to the naked eye. The superlattice structures observed by electron microscopy showed the periodic organization and packing between the individual particles into a continuously layered frame over long length scales. The photonic PbSe films were used to design solid-state devices through incorporating them onto quartz substrates prepatterned with gold electrodes for measuring photoconductivity. The electrical transport measurements revealed the conductivity along the stripe direction was 20 times larger than that in the direction perpendicular to stripes, which was determined by the ordered superlattices.

Semiconductor films derived from self-organizing the quantum dots into macroscopic assemblies were reported by Urban *et al.*[166] Monodisperse, defect-free PbTe nanocrystals with narrow size distributions were prepared from hot injection and size-selective process. Densely packed nanocrystal superlattice glassy films over long length scales were formed by drop-casting PbTe nanocrystal dispersion on Si/SiO_2 substrates. The thin film semiconductor devices were tested for conductive properties. The organic–inorganic hybrid films showed a poor conductivity resulting from the difficulty of the charge transport associated with the large interparticle separation of the capping organic

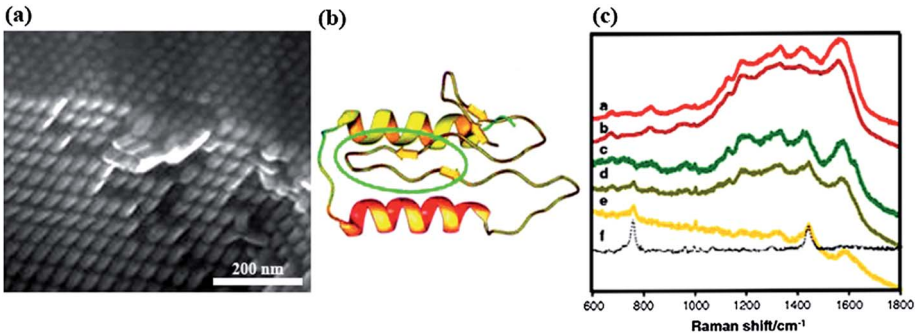

Fig. 18 Gold superlattices as SERS spectroscopy substrates for selective detection of prion protein. (a) SEM image viewed along the edge of gold nanorod superlattices. (b) Scheme showing prion mutation for biologically active β-sheet prions with 106–126 peptide fragments presented in green. (c) SERS spectra of different samples going from a to f corresponding to natural human blood, spiked human blood, natural human plasma, spiked human plasma, spiked human plasma after spectral subtraction of human plasma matrix, and scrambled prion. Reproduced with permission from ref. 168. Copyright 2010 Proceedings of the National Academy of Sciences.

ligands. Thus, the chemical activation of these films by hydrazine was carried out to decrease the interparticle spacing through the removal of the oleic acid groups. Patterning of the nanocrystal solids after treatment exhibited an enhanced conductance compared to the untreated films. In an another report, a collective plasmonic response of tunable plasmonic coupling in densely packed binary superlattices from plasmonic and nonplasmonic nanocrystal assemblies was demonstrated.[167] This highlights the unprecedented control over peak reflected wavelength across the entire visible spectrum, offering applications for emerging optical elements.

The plasmonic superstructures with new collective properties offer additional advantages for bioanalysis making possible quantitative SERS detection of complex biomolecules.[169] Fig. 18 shows the self-organization of the gold nanorods into highly ordered superstructures supported on films reported by Alvarez-Puebla *et al.*[168] The gold superlattice films exhibited a plasmonic enhancement of electrical field, thus they can function as SERS substrates for sensitive detection of prion protein within complex biological media. The dilute solution of the prions prepared in NaCl, KCl, and phosphate buffer salts and human blood containing prions with low concentration were cast each onto the gold superstructure films. SERS spectroscopy of the superstructure-loaded samples, particularly for direct analysis of the contaminated human blood samples showed an enhanced intensity of bands characteristic of the binding of the peptide to the gold supercrystal surface. The authors pointed out that the intensity of SERS signal for the prion detection can be ultrasensitive to the prion concentration of as low as 10^{-10} M. It is important to bear in mind that the rational design of these SERS bioprobes with high sensitivity offer practical uses of direct and fast response of the prion infection within both *in vitro* and *in vivo* biological experiments.

Materials researchers believe that such responsive superlattice materials provide new platforms for the fabrication of novel opto-electronic sensors. The optical responses of such superlattices to the variation of the external environment are effective to be fast and fully reversible opto-electronic response, which may be of potential use in switches, patterns, and photoconductivities.

6. Summary and outlook

This review has provided an overview of recent progress in the interesting and developing scope of multifunctional organic-conjugated inorganic hybrid nanostructures with hierarchical geometries. This subject presents an interdisciplinary advance to couple unique opto-electronic properties of the single components in a hybrid system. The similarity of the nanometer dimensions of the inorganic particles and biomolecules, such as DNA, antibodies, or peptides, makes the functional hybrid systems as promising building blocks for the design of optical sensing and cancer diagnostic tools at the nanoscale.

Perspectives of multicomponent nanoarchitectures have been mentioned, including collective properties arising from clever multicomponent combinations and potential applications in photoswitchable, analytical, and biomedical fields. Although some applied branches have shown viable technologies, most of the others still represent an embryonic stage and need further research. Developing the sensing and biomedical diagnostic applications of nanocomposites have been the subject of tremendous research efforts over the last years. The firm grasp on the unique opto-electronic properties of the inorganic particles and bioactivity of the biomolecule linkers has enabled them to combine into photophysic interparticle nanoarchitectures that can function as integrated optical probes for recognition and diagnostic processes.

The facile approaches for synthesizing multicomponent nanostructures with hierarchical geometries such as core–shell, dumbbell, chirality, photonic arrays have been presented. The core–shell and dumbbell-shaped nanohybrids were produced by sequential growth of secondary precursors on seeds through directed attachment. The single components, which have similar lattice facets, can fuse together to form a dumbbell hybrid, whereas a large difference of the lattice structure of the single components can lead to a phase separation of the components, forming a core–shell hybrid. The use of the biomaterials as templates for the generation of nanostructures and nanocircuitry in the presence of nanoparticles is in an early phase of development. DNA-functionalized plasmonic nanostructures are prepared by assembling metal clusters with

biomolecules or template of helical DNA *via* intermolecular hydrogen bonding and electrostatic interactions. Periodically nanocrystal arrays with tunable optical properties are constructed by orientating the surface-functionalized particle colloids into superlattice structures in response to application of an external magnetic field or slow solvent evaporation.

The biomolecule-conjugated plasmonic–magnetic, fluorescent–magnetic, and fluorescent-upconverting nanohybrids applied for MRI contrast and anticancer agent applications were discussed. The shape-controlled synergistic properties of the complex nanoarchitectures are integrated into biomolecule-conjugated particle composites offering simultaneously cancer therapeutic and diagnostic functions. As the plasmonic–magnetic nanostructures targeted onto the membrane of cancer tumors, the carriers of the plasmonic particles and magnetic particles release photothermal-generated heating to kill the cancer cells upon laser irradiation and externally applied magnetic field, respectively. The fluorescent–magnetic nanoprobes can visualize inside labeled cells due to the fluorescent emission, and kill the cancer tumors by photothermal conversion of the magnetic property. Alternatively, the fluorescent upconverting nanohybrids exhibit both emission-labelled bioprobes and cancer therapeutics by releasing reactive single oxygen species under near infrared light irradiation.

The assembly of DNA-functionalized plasmonic particles to develop optical sensors for selective electronic detection of biorecognition events was presented. The viability of the concept is proven, and helical structures of controlled shapes and electronic functions can be obtained by incorporating the particles on the template biomaterials. Plasmonic particles attached onto helical DNA nanobundles exhibit surface plasmon resonance and circular dichroism (CD) signals arising from the collective electron oscillation and chiral dipolar coupling of the surface plasmon resonance, respectively. Also, the plasmonic nanoparticles are accessible and show CD responses to adsorbed guests.

An emerging area of opto-electronic photoswitch patterns of the periodic nanocrystal arrays derived from orienting uniform nanocrystal assemblies were presented. The sensing approach is based on the utilization of the superlattices as tunable optical patterns capable of changing their refractive properties when in contact with an analyte of interest or when exposed to environmental responses. The superlattices with long-range ordering exhibit photonic iridescent colors and optical properties from visible light reflection. The photonic and optical response of such materials can be tuned by changing external stimuli. "Smart" nanocrystal superlattices are extended to other applications toward the design of label-free biological, chemical, and physical sensors.

Besides the successful synthesis of the interesting biomolecule-conjugated hybrid nanoarchitectures, the development of fundamental applications of these promising nanomaterials in the future still face major challenges with the design of visible sensing and diagnostic devices in nanotechnology and clinical practices. A synergistic combination of unexpected features of nanoobjects and biomaterials provides great potential for integrated collaboration between material scientists, biologists and clinicians, who together can realise the transfer of academic experiments to commercial nanobiotechnology.

Acknowledgements

TDN and THT are grateful to the Natural Sciences and Engineering Research Council of Canada and the National Foundation for Science and Technology development of Vietnam – no. 104.03-2012.54 for funding, respectively.

References

1 E. Katz and I. Willner, Integrated Nanoparticle–Biomolecule Hybrid Systems: Synthesis, Properties, and Applications, *Angew. Chem., Int. Ed.*, 2004, **43**(45), 6042–6108.
2 J. Z. Zhang, Biomedical Applications of Shape-Controlled Plasmonic Nanostructures: A Case Study of Hollow Gold Nanospheres for Photothermal Ablation Therapy of Cancer, *J. Phys. Chem. Lett.*, 2010, **1**(4), 686–695.
3 R. Costi, A. E. Saunders and U. Banin, Colloidal Hybrid Nanostructures: A New Type of Functional Materials, *Angew. Chem., Int. Ed.*, 2010, **49**(29), 4878–4897.
4 D. Barreca, A. Gasparotto and E. Tondello, Metal/oxide interfaces in inorganic nanosystems: what's going on and what's next?, *J. Mater. Chem.*, 2011, **21**(6), 1648–1654.
5 N. A. Frey, *et al.*, Magnetic nanoparticles: synthesis, functionalization, and applications in bioimaging and magnetic energy storage, *Chem. Soc. Rev.*, 2009, **38**(9), 2532–2542.
6 K. Saha, *et al.*, Gold Nanoparticles in Chemical and Biological Sensing, *Chem. Rev.*, 2012, **112**(5), 2739–2779.
7 Y. Wang, B. Yan and L. Chen, SERS Tags: Novel Optical Nanoprobes for Bioanalysis, *Chem. Rev.*, 2012, **113**(3), 1391–1428.
8 J. T. Shawn, *et al.*, Building plasmonic nanostructures with DNA, *Nat. Nanotechnol.*, 2011, **6**(5), 268–276.
9 T. Mokari, *et al.*, Selective Growth of Metal Tips onto Semiconductor Quantum Rods and Tetrapods, *Science*, 2004, **304**(5678), 1787–1790.
10 D. Wang and Y. Li, Bimetallic Nanocrystals: Liquid-Phase Synthesis and Catalytic Applications, *Adv. Mater.*, 2011, **23**(9), 1044–1060.
11 H. Zeng and S. Sun, Syntheses, Properties, and Potential Applications of Multicomponent Magnetic Nanoparticles, *Adv. Funct. Mater.*, 2008, **18**(3), 391–400.
12 C. Petr, *et al.*, DNA-controlled assembly of a NaTl lattice structure from gold nanoparticles and protein nanoparticles, *Nat. Mater.*, 2010, **9**(11), 918–922.
13 K. Anton, *et al.*, DNA-based self-assembly of chiral plasmonic nanostructures with tailored optical response, *Nature*, 2012, **483**(7389), 311–314.
14 L. Guerrini and D. Graham, Molecularly-mediated assemblies of plasmonic nanoparticles for Surface-Enhanced Raman Spectroscopy applications, *Chem. Soc. Rev.*, 2012, **41**(21), 7085–7107.

15 L. He, *et al.*, Magnetic Assembly Route to Colloidal Responsive Photonic Nanostructures, *Acc. Chem. Res.*, 2012, **45**(9), 1431–1440.
16 M. Grzelczak, *et al.*, Directed Self-Assembly of Nanoparticles, *ACS Nano*, 2010, **4**(7), 3591–3605.
17 S. Jiang, *et al.*, Surface-functionalized nanoparticles for biosensing and imaging-guided therapeutics, *Nanoscale*, 2013, **5**(8), 3127–3148.
18 J. Yang, *et al.*, Fluorescent magnetic nanohybrids as multimodal imaging agents for human epithelial cancer detection, *Biomaterials*, 2008, **29**(16), 2548–2555.
19 H. H. P. Yiu, *et al.*, Designed Multifunctional Nanocomposites for Biomedical Applications, *Adv. Funct. Mater.*, 2010, **20**(10), 1599–1609.
20 E.-Q. Song, *et al.*, Fluorescent-Magnetic-Biotargeting Multifunctional Nanobioprobes for Detecting and Isolating Multiple Types of Tumor Cells, *ACS Nano*, 2011, **5**(2), 761–770.
21 I. Niagara Muhammad, *et al.*, *In vivo* photodynamic therapy using upconversion nanoparticles as remote-controlled nanotransducers, *Nat. Med.*, 2012, **18**(10), 1580–1585.
22 M. K. G. Jayakumar, N. M. Idris and Y. Zhang, Remote activation of biomolecules in deep tissues using near-infrared-to-UV upconversion nanotransducers, *Proc. Natl. Acad. Sci. U. S. A.*, 2012, **109**(22), 8483–8488.
23 Y. Liu, *et al.*, Lanthanide-doped luminescent nanoprobes: controlled synthesis, optical spectroscopy, and bioapplications, *Chem. Soc. Rev.*, 2013, **42**(16), 6924–6958.
24 Y. Ke, *et al.*, Three-Dimensional Structures Self-Assembled from DNA Bricks, *Science*, 2012, **338**(6111), 1177–1183.
25 J. Sharma, *et al.*, Control of Self-Assembly of DNA Tubules Through Integration of Gold Nanoparticles, *Science*, 2009, **323**(5910), 112–116.
26 M. R. Jones, *et al.*, Templated Techniques for the Synthesis and Assembly of Plasmonic Nanostructures, *Chem. Rev.*, 2011, **111**(6), 3736–3827.
27 J. Zhang, *et al.*, A gold nanoparticle-based chronocoulometric DNA sensor for amplified detection of DNA, *Nat. Protoc.*, 2007, **2**(11), 2888–2895.
28 L. Dong-Kwon, *et al.*, Highly uniform and reproducible surface-enhanced Raman scattering from DNA-tailorable nanoparticles with 1-nm interior gap, *Nat. Nanotechnol.*, 2011, **6**(7), 452–460.
29 M. S. Strano, Functional DNA Origami Devices, *Science*, 2012, **338**(6109), 890–891.
30 E. Ozbay, Plasmonics: Merging Photonics and Electronics at Nanoscale Dimensions, *Science*, 2006, **311**(5758), 189–193.
31 Z. Yu, C.-F. Wang and S. Chen, Fabrication of quantum dot-based photonic materials from small to large *via* interfacial self-assembly, *J. Mater. Chem.*, 2011, **21**(24), 8496–8501.
32 J. Ge, S. Kwon and Y. Yin, Niche applications of magnetically responsive photonic structures, *J. Mater. Chem.*, 2010, **20**(28), 5777–5784.
33 K. Shin-Hyun, *et al.*, Self-assembled colloidal structures for photonics, *NPG Asia Mater.*, 2011, **3**(1), 25–33.
34 B. Uri and S. Amit, Colloidal self-assembly: Superparticles get complex, *Nat. Mater.*, 2012, **11**(12), 1009–1011.
35 N. Erathodiyil and J. Y. Ying, Functionalization of Inorganic Nanoparticles for Bioimaging Applications, *Acc. Chem. Res.*, 2011, **44**(10), 925–935.
36 J. D. Joannopoulos, P. R. Villeneuve and S. Fan, Photonic crystals: putting a new twist on light, *Nature*, 1997, **386**(6621), 143–149.
37 A. Forchel, Photonic crystals: Switching light with light, *Nat. Mater.*, 2003, **2**(1), 13–14.
38 H. Benisty, Photonic crystals: New designs to confine light, *Nat. Phys.*, 2005, **1**(1), 9–10.
39 Y. Zhao, *et al.*, Bio-inspired variable structural color materials, *Chem. Soc. Rev.*, 2012, **41**(8), 3297–3317.
40 C. I. Aguirre, E. Reguera and A. Stein, Tunable Colors in Opals and Inverse Opal Photonic Crystals, *Adv. Funct. Mater.*, 2010, **20**(16), 2565–2578.
41 N. Huebsch and D. J. Mooney, Inspiration and application in the evolution of biomaterials, *Nature*, 2009, **462**(7272), 426–432.
42 F. Xia and L. Jiang, Bio-Inspired, Smart, Multiscale Interfacial Materials, *Adv. Mater.*, 2008, **20**(15), 2842–2858.
43 A. Polman and H. A. Atwater, Photonic design principles for ultrahigh-efficiency photovoltaics, *Nat. Mater.*, 2012, **11**(3), 174–177.
44 H. Kim, *et al.*, Structural colour printing using a magnetically tunable and lithographically fixable photonic crystal, *Nat. Photonics*, 2009, **3**(9), 534–540.
45 X. Huang, S. Neretina and M. A. El-Sayed, Gold Nanorods: From Synthesis and Properties to Biological and Biomedical Applications, *Adv. Mater.*, 2009, **21**(48), 4880–4910.
46 Z. Kyryl and C. W. C. Warren, Bioimaging: Illuminating the deep, *Nat. Mater.*, 2013, **12**(4), 285–287.
47 V. Biju, T. Itoh and M. Ishikawa, Delivering quantum dots to cells: bioconjugated quantum dots for targeted and nonspecific extracellular and intracellular imaging, *Chem. Soc. Rev.*, 2010, **39**(8), 3031–3056.
48 J. E. Lee, *et al.*, Multifunctional Mesoporous Silica Nanocomposite Nanoparticles for Theranostic Applications, *Acc. Chem. Res.*, 2011, **44**(10), 893–902.
49 J. Gao, H. Gu and B. Xu, Multifunctional Magnetic Nanoparticles: Design, Synthesis, and Biomedical Applications, *Acc. Chem. Res.*, 2009, **42**(8), 1097–1107.
50 M. J. Sailor and J.-H. Park, Hybrid Nanoparticles for Detection and Treatment of Cancer, *Adv. Mater.*, 2012, **24**(28), 3779–3802.
51 G.-P. Wang, *et al.*, Biofunctionalization of fluorescent-magnetic-bifunctional nanospheres and their applications, *Chem. Commun.*, 2005, (34), 4276–4278.
52 W. Yan, *et al.*, Self-Assembly of Chiral Nanoparticle Pyramids with Strong *R*/*S* Optical Activity, *J. Am. Chem. Soc.*, 2012, **134**(36), 15114–15121.
53 S. Y. Park, DNA-programmable nanoparticle crystallization, *Nature*, 2007, **451**(7178), 553–556.
54 J. Ge, *et al.*, Magnetochromatic Microspheres: Rotating Photonic Crystals, *J. Am. Chem. Soc.*, 2009, **131**(43), 15687–15694.

55 X. Ye, *et al.*, Improved Size-Tunable Synthesis of Monodisperse Gold Nanorods through the Use of Aromatic Additives, *ACS Nano*, 2012, **6**(3), 2804–2817.
56 X. Ye, *et al.*, Using Binary Surfactant Mixtures To Simultaneously Improve the Dimensional Tunability and Monodispersity in the Seeded Growth of Gold Nanorods, *Nano Lett.*, 2013, **13**(2), 765–771.
57 C. Gao, *et al.*, Templated Synthesis of Metal Nanorods in Silica Nanotubes, *J. Am. Chem. Soc.*, 2011, **133**(49), 19706–19709.
58 A. Walther and A. H. E. Müller, Janus Particles: Synthesis, Self-Assembly, Physical Properties, and Applications, *Chem. Rev.*, 2013, **113**(7), 5194–5261.
59 T. Mokari, *et al.*, Formation of asymmetric one-sided metal-tipped semiconductor nanocrystal dots and rods, *Nat. Mater.*, 2005, **4**(11), 855–863.
60 C.-T. Dinh, *et al.*, A New Route to Size and Population Control of Silver Clusters on Colloidal TiO_2 Nanocrystals, *ACS Appl. Mater. Interfaces*, 2011, **3**(7), 2228–2234.
61 E. V. Shevchenko, *et al.*, Gold/Iron Oxide Core/Hollow-Shell Nanoparticles, *Adv. Mater.*, 2008, **20**(22), 4323–4329.
62 H. Yu, *et al.*, Dumbbell-like Bifunctional Au–Fe_3O_4 Nanoparticles, *Nano Lett.*, 2005, **5**(2), 379–382.
63 T.-D. Nguyen, C.-T. Dinh and T.-O. Do, A general procedure to synthesize highly crystalline metal oxide and mixed oxide nanocrystals in aqueous medium and photocatalytic activity of metal/oxide nanohybrids, *Nanoscale*, 2011, **3**(4), 1861–1873.
64 T.-D. Nguyen, *et al.*, Controlled synthesis of ceria nanoparticles for the design of nanohybrids, *J. Colloid Interface Sci.*, 2013, **394**(0), 100–107.
65 C.-T. Dinh, *et al.*, Controlled Synthesis of Titanate Nanodisks as Versatile Building Blocks for the Design of Hybrid Nanostructures, *Angew. Chem., Int. Ed.*, 2012, **51**(27), 6608–6612.
66 S. Burge, *et al.*, Quadruplex DNA: sequence, topology and structure, *Nucleic Acids Res.*, 2006, **34**(19), 5402–5415.
67 H. Dietz, *et al.*, Self-assembly of DNA into nanoscale three-dimensional shapes, *Nature*, 2009, **459**(7245), 414.
68 Z. David Yu and G. Seelig, Dynamic DNA nanotechnology using strand-displacement reactions, *Nat. Chem.*, 2011, **3**(2), 103–113.
69 W. K. R. Paul, Folding DNA to create nanoscale shapes and patterns, *Nature*, 2006, **440**(7082), 297–302.
70 X. Ma, *et al.*, Molecular miscibility characteristics of self-assembled 2D molecular architectures, *J. Mater. Chem.*, 2008, **18**(18), 2074–2081.
71 S. A. Claridge, *et al.*, Cluster-Assembled Materials, *ACS Nano*, 2009, **3**(2), 244–255.
72 S. Kinge, M. Crego-Calama and D. N. Reinhoudt, Self-Assembling Nanoparticles at Surfaces and Interfaces, *ChemPhysChem*, 2008, **9**(1), 20–42.
73 K. S. Cho, *et al.*, Three-dimensional binary superlattices of magnetic nanocrystals and semiconductor quantum dots, *Nature*, 2003, **423**(6943), 968–971.
74 J. Ge, Y. Hu and Y. Yin, Highly Tunable Superparamagnetic Colloidal Photonic Crystals, *Angew. Chem., Int. Ed.*, 2007, **46**(39), 7428–7431.
75 J. Ge and Y. Yin, Magnetically Tunable Colloidal Photonic Structures in Alkanol Solutions, *Adv. Mater.*, 2008, **20**(18), 3485–3491.
76 X. Ye, *et al.*, Morphologically controlled synthesis of colloidal upconversion nanophosphors and their shape-directed self-assembly, *Proc. Natl. Acad. Sci. U. S. A.*, 2010, **107**(52), 22430–22435.
77 S. Umadevi, X. Feng and T. Hegmann, Large Area Self-Assembly of Nematic Liquid-Crystal-Functionalized Gold Nanorods, *Adv. Funct. Mater.*, 2013, **23**(11), 1393–1403.
78 R. H. Marchessault, F. F. Morehead and N. M. Walter, Liquid Crystal Systems from Fibrillar Polysaccharides, *Nature*, 1959, **184**(4686), 632–633.
79 X. Zhen and G. Chao, Graphene chiral liquid crystals and macroscopic assembled fibres, *Nat. Commun.*, 2011, **2**, 571.
80 G. L. Nealon, *et al.*, Liquid-crystalline nanoparticles: Hybrid design and mesophase structures, *Beilstein J. Org. Chem.*, 2012, **8**, 349–370.
81 J. C. Payne and E. L. Thomas, Towards an Understanding of Nanoparticle–Chiral Nematic Liquid Crystal Co-Assembly, *Adv. Funct. Mater.*, 2007, **17**(15), 2717–2721.
82 C. Wang, *et al.*, Recent Progress in Syntheses and Applications of Dumbbell-like Nanoparticles, *Adv. Mater.*, 2009, **21**(30), 3045–3052.
83 G. Menagen, *et al.*, Au Growth on Semiconductor Nanorods: Photoinduced *versus* Thermal Growth Mechanisms, *J. Am. Chem. Soc.*, 2009, **131**(47), 17406–17411.
84 E. M. Janet, *et al.*, Hybrid nanoscale inorganic cages, *Nat. Mater.*, 2010, **9**(10), 810–815.
85 M. Meyns, *et al.*, Growth and reductive transformation of a gold shell around pyramidal cadmium selenide nanocrystals, *J. Mater. Chem.*, 2010, **20**(47), 10602–10605.
86 S. Chakrabortty, *et al.*, Asymmetric Dumbbells from Selective Deposition of Metals on Seeded Semiconductor Nanorods, *Angew. Chem., Int. Ed.*, 2010, **49**(16), 2888–2892.
87 K.-W. Kwon and M. Shim, γ-Fe_2O_3/II–VI Sulfide Nanocrystal Heterojunctions, *J. Am. Chem. Soc.*, 2005, **127**(29), 10269–10275.
88 M. Liu and P. Guyot-Sionnest, Preparation and optical properties of silver chalcogenide coated gold nanorods, *J. Mater. Chem.*, 2006, **16**(40), 3942–3945.
89 C. Xu, *et al.*, Au–Fe_3O_4 Dumbbell Nanoparticles as Dual-Functional Probes, *Angew. Chem., Int. Ed.*, 2008, **47**(1), 173–176.
90 Z. Xu, Y. Hou and S. Sun, Magnetic Core/Shell Fe_3O_4/Au and Fe_3O_4/Au/Ag Nanoparticles with Tunable Plasmonic Properties, *J. Am. Chem. Soc.*, 2007, **129**(28), 8698–8699.
91 M. S. Yavuz, *et al.*, Gold nanocages covered by smart polymers for controlled release with near-infrared light, *Nat. Mater.*, 2009, **8**(12), 935–939.
92 S. E. Skrabalak, *et al.*, Gold Nanocages: Synthesis, Properties, and Applications, *Acc. Chem. Res.*, 2008, **41**(12), 1587–1595.

93 S. Lal, S. E. Clare and N. J. Halas, Nanoshell-Enabled Photothermal Cancer Therapy: Impending Clinical Impact, *Acc. Chem. Res.*, 2008, **41**(12), 1842–1851.
94 Y. Chen, *et al.*, Core/Shell Structured Hollow Mesoporous Nanocapsules: A Potential Platform for Simultaneous Cell Imaging and Anticancer Drug Delivery, *ACS Nano*, 2010, **4**(10), 6001–6013.
95 S.-H. Choi, *et al.*, Simple and Generalized Synthesis of Oxide–Metal Heterostructured Nanoparticles and their Applications in Multimodal Biomedical Probes, *J. Am. Chem. Soc.*, 2008, **130**(46), 15573–15580.
96 C.-H. Kuo, T.-E. Hua and M. H. Huang, Au Nanocrystal-Directed Growth of Au–Cu_2O Core–Shell Heterostructures with Precise Morphological Control, *J. Am. Chem. Soc.*, 2009, **131**(49), 17871–17878.
97 E. Wetterskog, *et al.*, Anomalous Magnetic Properties of Nanoparticles Arising from Defect Structures: Topotaxial Oxidation of $Fe_{1-x}O$–$Fe_{3-\delta}O_4$ Core–Shell Nanocubes to Single-Phase Particles, *ACS Nano*, 2013, **7**(8), 7132–7144.
98 P.-H. Chen, *et al.*, Direct Observation of Au/Ga_2O_3 Peapodded Nanowires and Their Plasmonic Behaviors, *Nano Lett.*, 2010, **10**(9), 3267–3271.
99 C. Cheng, *et al.*, HierarchicalAssembly of ZnO Nanostructures on SnO_2 Backbone Nanowires: Low-Temperature Hydrothermal Preparation and Optical Properties, *ACS Nano*, 2009, **3**(10), 3069–3076.
100 D. Wang and Y. Li, One-Pot Protocol for Au-Based Hybrid Magnetic Nanostructures *via* a Noble-Metal-Induced Reduction Process, *J. Am. Chem. Soc.*, 2010, **132**(18), 6280–6281.
101 V. Mazumder, *et al.*, Core/Shell Pd/FePt Nanoparticles as an Active and Durable Catalyst for the Oxygen Reduction Reaction, *J. Am. Chem. Soc.*, 2010, **132**(23), 7848–7849.
102 H. Zeng, *et al.*, Bimagnetic Core/Shell FePt/Fe_3O_4 Nanoparticles, *Nano Lett.*, 2003, **4**(1), 187–190.
103 Y. Ma, *et al.*, Au@Ag Core–Shell Nanocubes with Finely Tuned and Well-Controlled Sizes, Shell Thicknesses, and Optical Properties, *ACS Nano*, 2010, **4**(11), 6725–6734.
104 N. Liu, B. S. Prall and V. I. Klimov, Hybrid Gold/Silica/Nanocrystal-Quantum-Dot Superstructures: Synthesis and Analysis of Semiconductor–Metal Interactions, *J. Am. Chem. Soc.*, 2006, **128**(48), 15362–15363.
105 J. Xu, *et al.*, Large-Scale Synthesis and Phase Transformation of CuSe, $CuInSe_2$, and $CuInSe_2$/$CuInS_2$ Core/Shell Nanowire Bundles, *ACS Nano*, 2010, **4**(4), 1845–1850.
106 D. C. Lee, *et al.*, Infrared-Active Heterostructured Nanocrystals with Ultralong Carrier Lifetimes, *J. Am. Chem. Soc.*, 2010, **132**(29), 9960–9962.
107 Y. Sun and Y. Xia, Shape-Controlled Synthesis of Gold and Silver Nanoparticles, *Science*, 2002, **298**(5601), 2176–2179.
108 E. Johann, *et al.*, Powering the programmed nanostructure and function of gold nanoparticles with catenated DNA machines, *Nat. Commun.*, 2013, **4**, 2000.
109 J.-S. Lee, *et al.*, Silver Nanoparticle–Oligonucleotide Conjugates Based on DNA with Triple Cyclic Disulfide Moieties, *Nano Lett.*, 2007, **7**(7), 2112–2115.
110 G. P. Mitchell, C. A. Mirkin and R. L. Letsinger, Programmed Assembly of DNA Functionalized Quantum Dots, *J. Am. Chem. Soc.*, 1999, **121**(35), 8122–8123.
111 J. I. Cutler, *et al.*, Polyvalent Oligonucleotide Iron Oxide Nanoparticle "Click" Conjugates, *Nano Lett.*, 2010, **10**(4), 1477–1480.
112 X. Zhang, M. R. Servos and J. Liu, Instantaneous and Quantitative Functionalization of Gold Nanoparticles with Thiolated DNA Using a pH-Assisted and Surfactant-Free Route, *J. Am. Chem. Soc.*, 2012, **134**(17), 7266–7269.
113 X. Zhang, M. R. Servos and J. Liu, Ultrahigh Nanoparticle Stability against Salt, pH, and Solvent with Retained Surface Accessibility *via* Depletion Stabilization, *J. Am. Chem. Soc.*, 2012, **134**(24), 9910–9913.
114 J.-Y. Kim and J.-S. Lee, Synthesis and Thermally Reversible Assembly of DNA–Gold Nanoparticle Cluster Conjugates, *Nano Lett.*, 2009, **9**(12), 4564–4569.
115 B. Lee, *et al.*, DNA-programmable nanoparticle crystallization, *Nature*, 2008, **451**(7178), 553–556.
116 H. Li, *et al.*, DNA-Templated Self-Assembly of Protein and Nanoparticle Linear Arrays, *J. Am. Chem. Soc.*, 2003, **126**(2), 418–419.
117 L. Pik Kwan, *et al.*, Loading and selective release of cargo in DNA nanotubes with longitudinal variation, *Nat. Chem.*, 2010, **2**(4), 319–328.
118 R. J. Macfarlane, *et al.*, Nanoparticle Superlattice Engineering with DNA, *Science*, 2011, **334**(6053), 204–208.
119 Y. He, *et al.*, DNA-Templated Fabrication of Two-Dimensional Metallic Nanostructures by Thermal Evaporation Coating, *J. Am. Chem. Soc.*, 2011, **133**(6), 1742–1744.
120 M. Wei, *et al.*, Chiral plasmonics of self-assembled nanorod dimers, *Sci. Rep.*, 2013, **3**, 1934.
121 J. D. Le, *et al.*, DNA-Templated Self-Assembly of Metallic Nanocomponent Arrays on a Surface, *Nano Lett.*, 2004, **4**(12), 2343–2347.
122 J. Zheng, *et al.*, Two-Dimensional Nanoparticle Arrays Show the Organizational Power of Robust DNA Motifs, *Nano Lett.*, 2006, **6**(7), 1502–1504.
123 C. Wenlong, *et al.*, Free-standing nanoparticle superlattice sheets controlled by DNA, *Nat. Mater.*, 2009, **8**(6), 519–525.
124 J. Sharma, *et al.*, DNA-Templated Self-Assembly of Two-Dimensional and Periodical Gold Nanoparticle Arrays, *Angew. Chem., Int. Ed.*, 2006, **45**(5), 730–735.
125 L. A. Stearns, *et al.*, Template-Directed Nucleation and Growth of Inorganic Nanoparticles on DNA Scaffolds, *Angew. Chem., Int. Ed.*, 2009, **48**(45), 8494–8496.
126 W. Stöber, A. Fink and E. Bohn, Controlled growth of monodisperse silica spheres in the micron size range, *J. Colloid Interface Sci.*, 1968, **26**(1), 62–69.
127 L. He, *et al.*, Determination of Solvation Layer Thickness by a Magnetophotonic Approach, *ACS Nano*, 2012, **6**(5), 4196–4202.
128 H. Joel, *et al.*, Self-assembly of uniform polyhedral silver nanocrystals into densest packings and exotic superlattices, *Nat. Mater.*, 2011, **11**(2), 131–137.

129 R. Hao, *et al.*, Synthesis, Functionalization, and Biomedical Applications of Multifunctional Magnetic Nanoparticles, *Adv. Mater.*, 2010, **22**(25), 2729–2742.
130 E. Kim, *et al.*, Magnetic nanocomplexes and the physiological challenges associated with their use for cancer imaging and therapy, *J. Mater. Chem. B*, 2013, **1**(6), 729–739.
131 P. Caravan, *et al.*, Gadolinium(III) Chelates as MRI Contrast Agents: Structure, Dynamics, and Applications, *Chem. Rev.*, 1999, **99**(9), 2293–2352.
132 H. B. Na, I. C. Song and T. Hyeon, Inorganic Nanoparticles for MRI Contrast Agents, *Adv. Mater.*, 2009, **21**(21), 2133–2148.
133 P. Y. Kim, *et al.*, Wrap-bake-peel process for nanostructural transformation from beta-FeOOH nanorods to biocompatible iron oxide nanocapsules, *Nat. Mater.*, 2008, **7**(3), 242–247.
134 C. Xu, B. Wang and S. Sun, Dumbbell-like Au–Fe_3O_4 Nanoparticles for Target-Specific Platin Delivery, *J. Am. Chem. Soc.*, 2009, **131**(12), 4216–4217.
135 K. Cheng, *et al.*, Porous Hollow Fe_3O_4 Nanoparticles for Targeted Delivery and Controlled Release of Cisplatin, *J. Am. Chem. Soc.*, 2009, **131**(30), 10637–10644.
136 Z. Fan, *et al.*, Multifunctional Plasmonic Shell–Magnetic Core Nanoparticles for Targeted Diagnostics, Isolation, and Photothermal Destruction of Tumor Cells, *ACS Nano*, 2012, **6**(2), 1065–1073.
137 J.-H. Park, *et al.*, Micellar Hybrid Nanoparticles for Simultaneous Magnetofluorescent Imaging and Drug Delivery, *Angew. Chem., Int. Ed.*, 2008, **47**(38), 7284–7288.
138 W.-K. Oh, *et al.*, Cellular Uptake, Cytotoxicity, and Innate Immune Response of Silica–Titania Hollow Nanoparticles Based on Size and Surface Functionality, *ACS Nano*, 2010, **4**(9), 5301–5313.
139 S. T. Selvan, *et al.*, Synthesis of Silica-Coated Semiconductor and Magnetic Quantum Dots and Their Use in the Imaging of Live Cells, *Angew. Chem., Int. Ed.*, 2007, **46**(14), 2448–2452.
140 L.-L. Li, *et al.*, An Exceptionally Simple Strategy for DNA-Functionalized Up-Conversion Nanoparticles as Biocompatible Agents for Nanoassembly, DNA Delivery, and Imaging, *J. Am. Chem. Soc.*, 2013, **135**(7), 2411–2414.
141 C.-T. Chen, *et al.*, A Triantennary Dendritic Galactoside-Capped Nanohybrid with a ZnS/CdSe Nanoparticle Core as a Hydrophilic, Fluorescent, Multivalent Probe for Metastatic Lung Cancer Cells, *Adv. Funct. Mater.*, 2008, **18**(4), 527–540.
142 J. E. Lee, *et al.*, Uniform Mesoporous Dye-Doped Silica Nanoparticles Decorated with Multiple Magnetite Nanocrystals for Simultaneous Enhanced Magnetic Resonance Imaging, Fluorescence Imaging, and Drug Delivery, *J. Am. Chem. Soc.*, 2009, **132**(2), 552–557.
143 S. Santra, *et al.*, Synthesis of Water-Dispersible Fluorescent, Radio-Opaque, and Paramagnetic CdS:Mn/ZnS Quantum Dots: A Multifunctional Probe for Bioimaging, *J. Am. Chem. Soc.*, 2005, **127**(6), 1656–1657.
144 F. Wang and X. Liu, Recent advances in the chemistry of lanthanide-doped upconversion nanocrystals, *Chem. Soc. Rev.*, 2009, **38**(4), 976–989.
145 F. Zhang, *et al.*, Mesoporous Multifunctional Upconversion Luminescent and Magnetic "Nanorattle" Materials for Targeted Chemotherapy, *Nano Lett.*, 2011, **12**(1), 61–67.
146 K. J. Rakesh and S. Triantafyllos, Delivering nanomedicine to solid tumors, *Nat. Rev. Clin. Oncol.*, 2010, **7**(11), 653–664.
147 S. J. Tan, *et al.*, Building plasmonic nanostructures with DNA, *Nat. Nanotechnol.*, 2011, **6**(5), 268–276.
148 A. P. Robby and M. D. Joseph, Strategies in the design of nanoparticles for therapeutic applications, *Nat. Rev. Drug Discovery*, 2010, **9**(8), 615–627.
149 J. A. Fan, *et al.*, DNA-Enabled Self-Assembly of Plasmonic Nanoclusters, *Nano Lett.*, 2011, **11**(11), 4859–4864.
150 D.-K. Lim, *et al.*, Highly uniform and reproducible surface-enhanced Raman scattering from DNA-tailorable nanoparticles with 1-nm interior gap, *Nat. Nanotechnol.*, 2011, **6**(7), 452–460.
151 D.-K. Lim, I.-J. Kim and J.-M. Nam, DNA-embedded Au/Ag core–shell nanoparticles, *Chem. Commun.*, 2008, (42), 5312–5314.
152 Y. Yan, J. I. L. Chen and D. S. Ginger, Photoswitchable Oligonucleotide-Modified Gold Nanoparticles: Controlling Hybridization Stringency with Photon Dose, *Nano Lett.*, 2012, **12**(5), 2530–2536.
153 R. J. Matthew, *et al.*, DNA-nanoparticle superlattices formed from anisotropic building blocks, *Nat. Mater.*, 2010, **9**(11), 913–917.
154 E. Dujardin, *et al.*, DNA-driven self-assembly of gold nanorods, *Chem. Commun.*, 2001, (14), 1264–1265.
155 Z. Li, *et al.*, Reversible Plasmonic Circular Dichroism of Au Nanorod and DNA Assemblies, *J. Am. Chem. Soc.*, 2012, **134**(7), 3322–3325.
156 S. Pal, *et al.*, DNA-Origami-Directed Self-Assembly of Discrete Silver-Nanoparticle Architectures, *Angew. Chem., Int. Ed.*, 2010, **49**(15), 2700–2704.
157 B. Ding, *et al.*, Gold Nanoparticle Self-Similar Chain Structure Organized by DNA Origami, *J. Am. Chem. Soc.*, 2010, **132**(10), 3248–3249.
158 J. K. Ryan, *et al.*, Placement and orientation of individual DNA shapes on lithographically patterned surfaces, *Nat. Nanotechnol.*, 2009, **4**(9), 557–561.
159 S. Pal, *et al.*, DNA Directed Self-Assembly of Anisotropic Plasmonic Nanostructures, *J. Am. Chem. Soc.*, 2011, **133**(44), 17606–17609.
160 G. P. Acuna, *et al.*, Fluorescence Enhancement at Docking Sites of DNA-Directed Self-Assembled Nanoantennas, *Science*, 2012, **338**(6106), 506–510.
161 J. H. Moon and S. Yang, Chemical Aspects of Three-Dimensional Photonic Crystals, *Chem. Rev.*, 2009, **110**(1), 547–574.
162 J. Kim, *et al.*, Lithographic compartmentalization of emulsion droplet templates for microparticles with multiple nanostructured compartments, *Chem. Commun.*, 2012, **48**(49), 6091–6093.

163 L. He, *et al.*, Magnetic Assembly and Patterning of General Nanoscale Materials through Nonmagnetic Templates, *Nano Lett.*, 2012, **13**(1), 264–271.
164 M. Wang, *et al.*, Magnetically rewritable photonic ink based on superparamagnetic nanochains, *J. Mater. Chem. C*, 2013, **1**(38), 6151–6156.
165 L. He, *et al.*, Magnetic Assembly of Nonmagnetic Particles into Photonic Crystal Structures, *Nano Lett.*, 2010, **10**(11), 4708–4714.
166 J. J. Urban, *et al.*, Self-Assembly of PbTe Quantum Dots into Nanocrystal Superlattices and Glassy Films, *J. Am. Chem. Soc.*, 2006, **128**(10), 3248–3255.
167 X. Ye, *et al.*, Tunable Plasmonic Coupling in Self-Assembled Binary Nanocrystal Superlattices Studied by Correlated Optical Microspectrophotometry and Electron Microscopy, *Nano Lett.*, 2013, **13**(3), 1291–1297.
168 R. A. Alvarez-Puebla, *et al.*, Gold nanorods 3D-supercrystals as surface enhanced Raman scattering spectroscopy substrates for the rapid detection of scrambled prions, *Proc. Natl. Acad. Sci. U. S. A.*, 2011, **108**(20), 8157–8161.
169 S. Lal, *et al.*, Tailoring plasmonic substrates for surface enhanced spectroscopies, *Chem. Soc. Rev.*, 2008, **37**(5), 898–911.

